PLOS ONE

RESEARCH ARTICLE

Identification of host genomic biomarkers from multiple transcriptomics datasets for diagnosis and therapies of SARS-CoV-2 infections

Bandhan Sarker[1,2☯], Md. Matiur Rahaman[1]*, Md. Ariful Islam[2☯], Muhammad Habibulla Alamin[1], Md. Maidul Husain[1], Farzana Ferdousi[1], Md. Asif Ahsan[2,3], Md. Nurul Haque Mollah[2]*

1 Faculty of Science, Department of Statistics, Bangabandhu Sheikh Mujibur Rahman Science and Technology University, Gopalganj, Bangladesh, **2** Department of Statistics, Bioinformatics Laboratory (Dry), University of Rajshahi, Rajshahi, Bangladesh, **3** Liangzhu Laboratory, Zhejiang University Medical Center, Zhejiang University, Hangzhou, Zhejiang, China

☯ These authors contributed equally to this work.
* matiur.stat@gmail.com (MMR); mollah.stat.bio@ru.ac.bd (MNHM)

Citation: Sarker B, Rahaman M.M, Islam M.A, Alamin MH, Husain M.M, Ferdousi F, et al. (2023) Identification of host genomic biomarkers from multiple transcriptomics datasets for diagnosis and therapies of SARS-CoV-2 infections. PLoS ONE 18(3): e0281981. https://doi.org/10.1371/journal.pone.0281981

Editor: Chandrabose Selvaraj, Alagappa University, INDIA

Received: October 6, 2022

Accepted: February 5, 2023

Published: March 13, 2023

Data Availability Statement: All relevant data are within the paper and its Supporting Information files.

Funding: This work was supported by the Ministry of Science and Technology Research Project (Ref: 505-ID, 2021–2022), Government of Bangladesh. The funders had no role in study design, data collection and analysis, decision to publish, or preparation of the manuscript.

Abstract

The pandemic of COVID-19 is a severe threat to human life and the global economy. Despite the success of vaccination efforts in reducing the spread of the virus, the situation remains largely uncontrolled due to the random mutation in the RNA sequence of severe acute respiratory syndrome coronavirus 2 (SARS-CoV-2), which demands different variants of effective drugs. Disease-causing gene-mediated proteins are usually used as receptors to explore effective drug molecules. In this study, we analyzed two different RNA-Seq and one microarray gene expression profile datasets by integrating EdgeR, LIMMA, weighted gene co-expression network and robust rank aggregation approaches, which revealed SARS-CoV-2 infection causing eight hub-genes (HubGs) including HubGs; *REL*, *AURKA*, *AURKB*, *FBXL3*, *OAS1*, *STAT4*, *MMP2* and *IL6* as the host genomic biomarkers. Gene Ontology and pathway enrichment analyses of HubGs significantly enriched some crucial biological processes, molecular functions, cellular components and signaling pathways that are associated with the mechanisms of SARS-CoV-2 infections. Regulatory network analysis identified top-ranked 5 TFs (SRF, PBX1, MEIS1, ESR1 and MYC) and 5 miRNAs (hsa-miR-106b-5p, hsa-miR-20b-5p, hsa-miR-93-5p, hsa-miR-106a-5p and hsa-miR-20a-5p) as the key transcriptional and post-transcriptional regulators of HubGs. Then, we conducted a molecular docking analysis to determine potential drug candidates that could interact with HubGs-mediated receptors. This analysis resulted in the identification of top-ranked ten drug agents, including Nilotinib, Tegobuvir, Digoxin, Proscillaridin, Olysio, Simeprevir, Hesperidin, Oleanolic Acid, Naltrindole and Danoprevir. Finally, we investigated the binding stability of the top-ranked three drug molecules Nilotinib, Tegobuvir and Proscillaridin with the three top-ranked proposed receptors (AURKA, AURKB, OAS1) by using 100 ns MD-based MM-PBSA simulations

Competing interests: The authors have declared that no competing interests exist.

and observed their stable performance. Therefore, the findings of this study might be useful resources for diagnosis and therapies of SARS-CoV-2 infections.

Introduction

The Severe Acute Respiratory Syndrome Coronavirus 2 (SARS-CoV-2), a highly contagious virus, has resulted in significant loss of human life. It first emerged in Wuhan, Hubei, China in December 2019, and rapidly spread throughout the world. The World Health Organization (WHO) has declared this outbreak a pandemic for the human community [1]. The global healthcare system has been tarnished by this pandemic. As per the WHO report, as of 23 September 2022, there have been 6,512,438 reported fatalities out of a total of 611,421,786 confirmed SARS-CoV-2 infections worldwide. Clinical investigations characterized SARS-CoV-2 infections as acute respiratory tract infections with versatile symptoms, including fever, cough, fatigue, shortness of breath and pneumonia [2]. Despite the fact that the symptoms of SARS-CoV-2 infections are almost known, preventive cures for SARS-CoV-2 infections are not yet at a satisfactory level [3–6]. Early detection of SARS-CoV-2 infections and its treatment with effective drugs may play a vital role to control its outspread [7,8]. Despite the availability of a variety of vaccines against SAR-CoV-2, including those from Pfizer, CoronaVac, BBIBP-CorV, AstraZeneca, BBV152, Moderna, Sputnik, EpiVacCorona, Ad5-nCoV, and WIBP [1,2], scientists and virologists around the world are anxious yet about their effectiveness due to the unstable virus RNA sequence patterns. So, they are continuing their research to understand the molecular mechanism of SARS-CoV-2 infections more clearly for finding effective cures. SARS-CoV-2 infections are developed with the mechanisms of genetic factors and host immune responses [9–11]. Thus, exploring the significant genomic biomarkers, underlying pathogenetic mechanisms and associated drug agents may hold the potential to provide a comprehensive understanding of SARS-CoV-2 infections, and ultimately leading to the discovery of efficacious diagnostic and therapeutic strategies.

Diseases-causing genes are widely used to explore pathogenetic processes and effective drug molecules. Several individual studies explored SARS-CoV-2 infections causing host genomic biomarkers, and their pathogenetic processes based on a single transcriptomics dataset [5,6,12–16]. We reviewed their articles and did not find any common infection-causing genes. Nevertheless, difficulties may arise during the plan to take standard treatment for all against infections of SARS-CoV-2 based on their infection-causing uncommon gene-guided drugs. Therefore, more representative SARS-CoV-2 infections causing genes must be explored for diagnosis and therapies.

Advanced high-throughput technologies are now producing large-scale transcriptome data (RNA-Seq and microarray). So, it has required novel procedures to figure out the consequential information. Integrated bioinformatics and statistical approaches are widely used to develop a novel pipeline for selecting more representative diseases causing genes [17,18]. Weighted gene co-expression network analysis (WGCNA) and robust rank aggregation (RRA) are two powerful cross-validation procedures for exploring the unseen interaction between insight of gene modules and gene samples [19–21]. Therefore, in this study, an attempt was made to explore (i) more representative SARS-CoV-2 infections causing key genes from a transcriptomics profile by cross-validation with the other two independent transcriptomics profiles, (ii) pathogenetic processes and regulatory components of key genes and (iii) key genes guided potential candidate drug agents for the treatment against infections of SARS-CoV-2.

Materials and methods

This study analyzed three transcriptomics datasets and associated meta-data on SARS-CoV-2 infections that are freely available in online sources by using integrated statistics and bioinformatics approaches. The workflow of this study is displayed in Fig 1 and described in the following sections.

Dataset acquisition and preprocessing

In this study, two RNA-Seq count datasets (GSE152418 and GSE147507), and one microarray dataset (GSE152075) of SARS-CoV-2 (COVID-19) were downloaded from the publicly available gene expression omnibus (GEO) database. GSE152418 raw count data contained 17

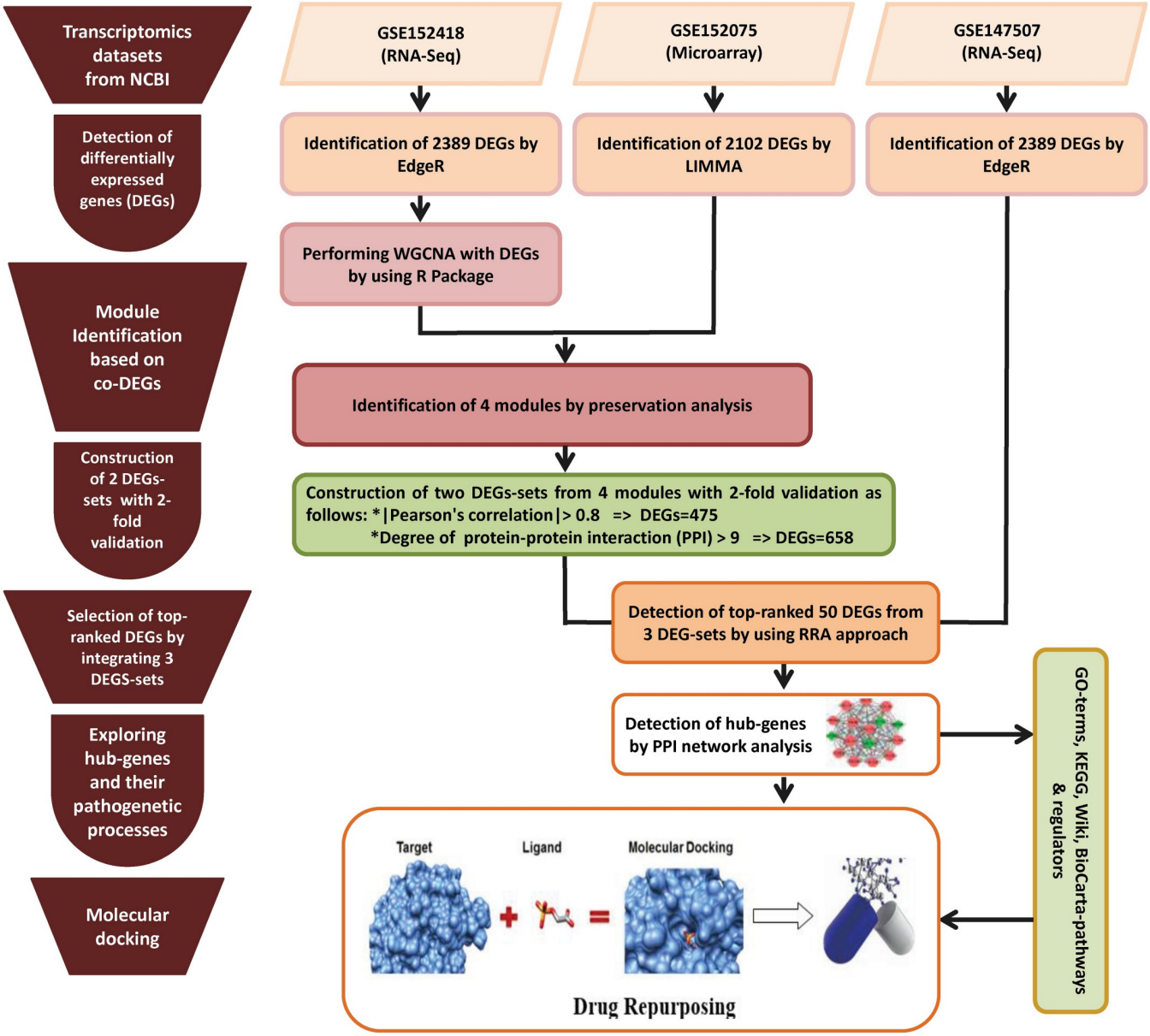

Fig 1. Workflow of the study.

https://doi.org/10.1371/journal.pone.0281981.g001

COVID-19 and 17 healthy samples [14,22]. GSE147507 raw count data contained 6 samples (3 COVID-19 patients and 3 NHBE samples) [15,23]. GSE152075 is a microarray data containing 430 COVID-19 infected samples and 54 negative samples [16,24–26]. The microarray dataset GSE152075 was downloaded using the Bioconductor package *GEOquery*, and the batch effect of this dataset was removed by using the R package *sva* via Combat_seq [27,28]. GSE152418 is used as a discovery dataset analyzed by WGCNA, GSE147507 is used as an independent validation, and GSE152075 is used as a test dataset. In the COVID-19 datasets, genes that comprise only zero counts have been removed.

Identification of differentially expressed genes (DEGs)

Differentially expressed genes (DEGs) were identified from the two RNA-Seq count datasets (GSE152418 and GSE147507) through *edgeR R*-package [16], and a microarray dataset (GSE152075) through *limma* R-package [29]. Genes were selected as DEGs that satisfy the criteria of adjusted P-value (Benjamini-Hochberg) < 0.05 and $|\log2\ (FC)| \geq 1$.

Weighted gene co-expression network analysis (WGCNA) with DEGs

The WGCNA approach was used for exploring modules (clusters) of highly correlated DEGs, summarizing such modules using the cluster eigengene or an intracluster hub genes, relating clusters to each other and to external sample traits (using eigengene networking), and for detecting cluster membership. We implemented this approach using the WGCNA *R* package [30]. In WGCNA, the *pickSoftThreshold* function was used for fitting soft-thresholding powers β over the value of maximum R^2. Then adjacency matrix and Topological Overlap Matrix (TOM) were created using TOM similarity. The dissimilarity of TOM (dissTOM) was computed using dissimilarity modules. Modules constructions of DEGs were performed using the *hclust* function from the dissTOM based dynamic cut tree (dendrogram). Different parameters were used for preventing large and small modules *i.e.*, medium sensitivity (*deepSplit* = 2) and minimum module size (*minClusterSize* = 30). Module eigengene (ME) was used for merging similar modules based on *MEDissThres* = 0.25 function.

Module analysis for validation of DEGs

To find the significant module of co-expressed DEGs (obtained through the WGCNA by integration of test dataset GSE152075), the module preservation function was used. The *module preservation function* is used to identify whether a module is reproducible and robust across the datasets or not [31]. We considered the module to be preserved if the statistic satisfied above Z summary > 10. It is specified negative correlation between preservation statistic-median rank and module preservation, and there is a positive correlation between the module preservation and Z summary statistic. Then the host DEGs were identified based on 2-fold cross-validation namely module membership statistic (MMS) calculated by the Pearson's correlation and Protein-protein interaction networks (PPIN). Genes of MMS, PPIN and DEGs from independent datasets were chosen as host signatures by RRA. The final subsets of host hub DEGs were separated by PPIN analysis (Fig 1).

Protein-protein interaction (PPI) network analysis based on validated DEGs

We performed PPI network analysis to explore SARS-CoV-2 infection causing hub-genes. To construct the PPI network for host signatures, genes data were collected from the STRING database [32], and the Cytoscape software [33] was used to construct the network based on the

parameter: confidence score ≥ 0.4 and most extreme interactors = 0 for cutoff models. Similarly, the hub-genes signatures were separated. After that, these hub signatures were used for gene enrichment analysis, finding transcriptional and post transcriptional regulators and drug repurposing with molecular docking analysis described in the next section.

Functional enrichment analysis of hub-genes

The Gene Ontology (GO), Kyoto Encyclopedia of Genes and Genomes (KEGG), WikiPathways and BioCarta pathway enrichment analyses for hub-genes were performed via the web-based tool *Enrichr* [34] to explore the pathogenetic processes of SARS-CoV-2 infections. P-value (Adjusted) < 0.05 was used to extract the significant biological information.

Hub-genes regulatory network analysis

To explore transcriptional and post-transcriptional regulators of hub-genes, we performed transcription factors (TFs) versus hub genes and micro RNAs versus hub genes interaction by using the databases TF2DNA [35] and miRDB [36], respectively.

Meta-data collection

We collected 177 drug agents as a meta-data from the literature review of 16 COVID-19 related articles to explore the potential candidate drugs (S1 Table). To validate the proposed repurposed candidate drugs by using molecular docking (MD) analysis with the top-ranked receptor proteins associated with COVID-19, the metadata were obtained from the literature review (S2 Table). We selected top-ranked COVID-19 associated 8 receptor proteins as meta-data by reviewing 24 newly published articles to assess the binding affinity of the proposed candidate drugs with these receptor proteins (S2 Table).

Molecular docking

To explore repurposable effective drug molecules for COVID-19 by *in-silico validation*, molecular docking analysis was performed between the target proteins and meta-drug agents. Our proposed HubGs mediated proteins and their associated TFs proteins were considered the drug target receptors, and 177 meta-drugs as the drug-agents that were obtained from the literature review and other sources as mentioned earlier in the data sources (S1 Table). From Protein Data Bank (PDB) [37] and SWISS-MODEL [38], the 3-Dimensional (3D) structures of receptor proteins were downloaded. The PubChem database [39] was used to download the 3D structures of drug agents. The PyMOL 2.4.1 software was used to visualize the 3D structure of the target receptor proteins [40]. The protein chains which were not a part of the gene are deleted [41]. Then, Swiss PDB viewer software was used to add charges and minimize the energy of the target proteins [42]. The target proteins were prepared for molecular docking analysis by eliminating water molecules and ligand heteroatoms, adding polar hydrogens, and converting them to pdbqt format using AutoDock tools 1.5.7 [43]. Avogadro software was used for minimizing the energy of the ligands [44]. The ligands were prepared for dynamic simulation by setting the torsion tree and rotatable, and nonrotatable bonds present in the ligand through AutoDock tools 1.5.7 [43]. Then, the binding affinities score between the ligand and receptors were calculated by using AutoDock Vina [45]. The Discovery Studio Visualizer 2019 was used to analyze the docked complexes. Let $\boldsymbol{S}_{ij}$ indicates the binding score of i^{th} receptors ($i = 1, 2, \ldots, m$) with the j^{th} ligand ($j = 1, 2, \ldots, n$). Then receptors were ordered according to the decreasing order of row means $\sum_{j=1}^{n} \boldsymbol{S}_{ij}/n;\ i = 1, 2, \ldots, m$ and ligands were ordered

according to the decreasing order of column means $\sum_{i=1}^{m} \boldsymbol{S}_{ij}/m;\ j = 1, 2, \ldots, n$ to select the top-order ligands as the candidate drug agents [5,17,46].

Molecular Dynamics (MD) simulation

To perform the dynamic properties of top-ordered protein-ligand complexes, YASARA [47] and the AMBER14 force field [48] were used in Molecular Dynamics (MD) simulations. We assigned the ligands parameters for the complexes by using AutoSMILES [49] algorithms, which automatically parameterize unknown organic molecules by computing semi-empirical AM1 Mulliken point charges with the COSMO solvation model, assigning AM1BCC [50] atom and bond types, and assigning general AMBER force field (GAFF) [51] atom types, and the remaining parameters of force field. In a simulation cell, the hydrogen bonding network of protein-ligand complexes were optimized and solvated by a TIP3P [52] water model before the simulation. We considered the solvent density of 0.997 g L^{-1} to maintain the periodic boundary conditions. During solvation, titratable amino acids in the protein complex were assigned to calculate pKa. The initial energy minimization process of each simulation system, consisting of 53735, 54335, and 79559 atoms for AURKA *vs*. Nilotinib, AURKB *vs*. Tegobuvir, and OAS1 *vs*. Proscillaridin complexes was performed by a simulated annealing method, respectively using the steepest gradient approach (5000 cycles).

A multiple-time-step algorithm [53] with 2.50 fs time step interval under physiological conditions (298 K, pH 7.4, 0.9% NaCl) [54] was used to run the simulation of each complex. The linear constraint solver (LINCS) [55] algorithm was used to constrain all bond lengths, and SETTLE [56] was employed to control the water molecules. PME methods [57] were used to describe long-range electrostatic interactions, and 100 ns MD simulation was performed at Berendsen thermostat [58] and constant pressure. The trajectories were captured at every 250 ps for further analysis, and subsequent analysis was performed by the built-in script of the YASARA [59] macro and SciDAVis software (http://scidavis.sourceforge.net/). All the captured snapshots were used to calculate MM-Poisson–Boltzmann Surface Area (MM-PBSA) binding free energy by YASARA software using the formula below [60]:

$$\text{Binding free energy} = (E_{\text{potReceptor}} + E_{\text{solvReceptor}} + E_{\text{potLigand}} + E_{\text{solvLigand}}) - (E_{\text{potComplex}} + E_{\text{solvComplex}})$$

Here, we computed MM-PBSA binding energy by YASARA default macros using AMBER 14 as a force field, with larger positive energies indicating better binding [61].

Results

Identification of DEGs

Two different raw RNA-Seq datasets (GSE152418 and GSE147507) and one microarray gene expression profile (GSE152075) were used for differential expression analysis (Table 1). We identified 2389 DEGs with 636 up-regulated and 1753 down-regulated genes for the GSE152418 dataset, and 540 DEGs with 213 up-regulated and 327 down-regulated genes for the GSE147507 dataset. We also identified 2102 DEGs with 570 up-regulated and 1532 down-regulated genes for GSE152075. These identified DEGs are used for further analysis.

WGCNA analysis for validation of DEGs

WGCNA was performed with the DEGs in the dataset GSE152418. The power value is the most important parameter which is contaminated with the average connectivity degree (ACD) and independence of co-expression modules (ICEM). The power value (Fig 2A) shows that

Table 1. Data description.

Datasets	DE genes		Total samples	COVID-19 samples	Normal samples
	Up- regulated	Down- regulated			
GSE152418	636	1753	34	17	17
GSE147507	213	327	6	3	3
GSE152075	570	1532	484	430	54

https://doi.org/10.1371/journal.pone.0281981.t001

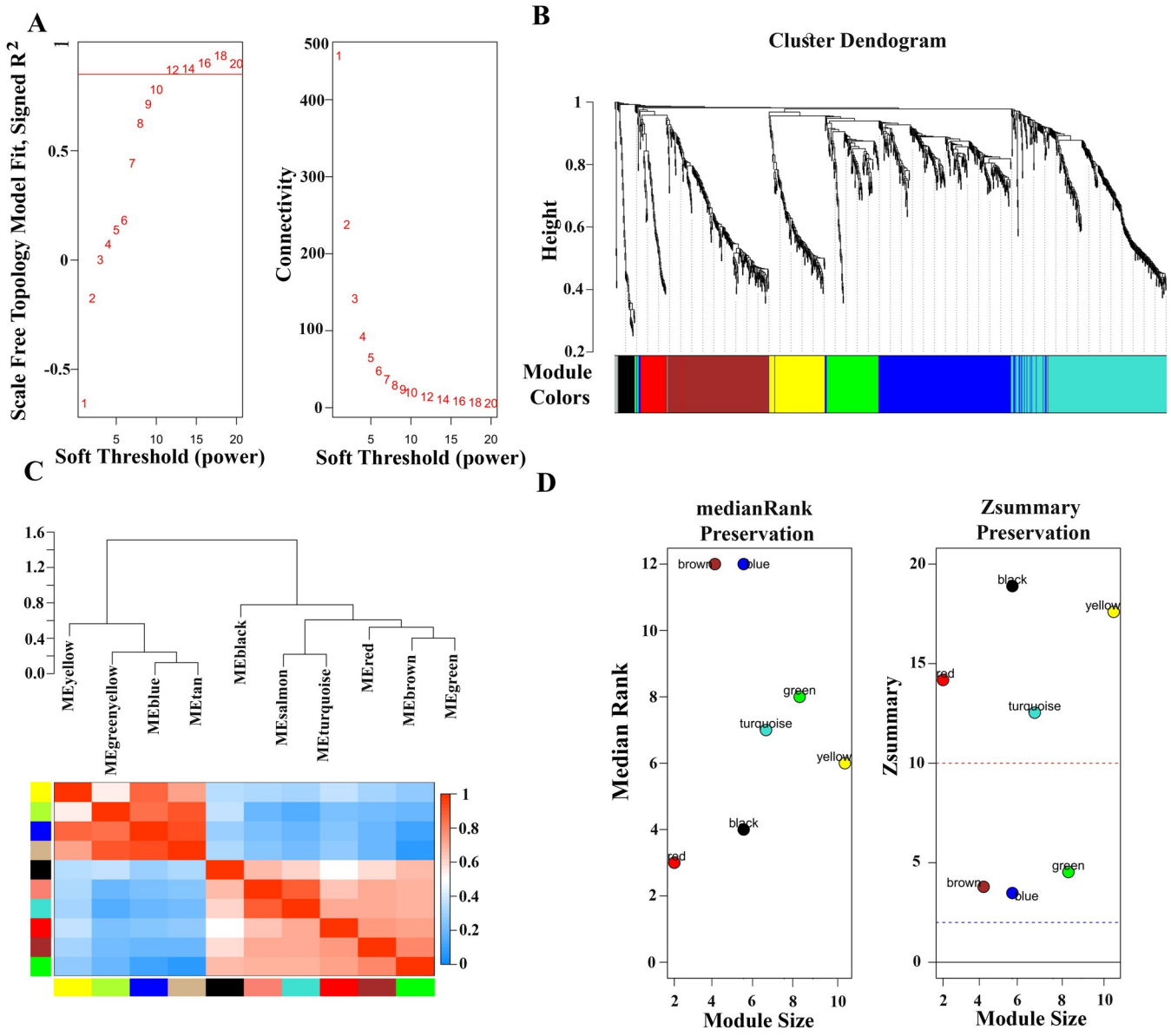

Fig 2. Cross-validation of DEGs by WGCNA. (A) Illustration of soft-thresholding powers based on the scale-free tropology model fit (left) and the mean connectivity (right). (B) The dendrogram of all DEGs clustered based on a dissimilarity measure (1-TOM). (C) The dendrogram of eigengene module and cluster analysis of eigengene network by heatmap summarize the modules yielded in the clustering analysis. (D) Median rank preservation (left) and Z summary preservation (Right); the black, red, yellow and turquoise indicate the strong preservation above dashed lines Z = 2 and Z = 10.

https://doi.org/10.1371/journal.pone.0281981.g002

ACD was greater, and the value of ICEM reached the expected value 0.8. Thus, the power value is ready to create the co-expression module and constructed with multiple colors presented in Fig 2B. The co-expression network constructed seven modules, namely black, red, yellow, turquoise, green, brown and blue, based on the soft threshold power $\beta = 6$ with $R^2 = 0.80$. The Eigengene dendrogram and eigengene network heatmap represent the interactions among the co-expression modules (Fig 2C). Then the dataset GSE152418 was compared with the test dataset GSE152075, and the summary of preservation statistic was visualized (Fig 2D). We observed that among the seven modules black, red, yellow and turquoise are the most stable modules (Zsummary statistic: above $Z = 2$ and $Z = 10$). The remaining modules were considered nonstable (Z summary statistic < 10). Black, red, yellow, and turquoise colors showed minimum median rank statistic which indicated that their preservation is best than the other modules.

Identification of hub-genes from validated DEGs

We identified 475 significant genes using high connectivity modules black, red, yellow and turquoise through the threshold |cor.geneModuleMembership| > 0.8. Again, the PPI network extracted 658 significant genes based on the highest degree > 9 for the four modules. These two gene sets were validated using the validation DEGs set. Validation DEGs set obtained from the GSE147507 dataset to confirm the most stable gene set of COVID-19. We used RRA to identify the top 50 significant genes in this case. Finally, eight hub genes (*REL*, *AURKA*, *AURKB*, *FBXL3*, *OAS1*, *STAT4*, *MMP2* and *IL6*) are identified from the top 50 genes through the PPI network analysis (Fig 3).

Functional enrichment analysis of hub-genes

Various pathway enrichment analyses were performed to explore further biological insight of the HubGs. GO and pathway terms with P-value (adjusted) < 0.05 were considered significant. The information of GO with their three subsections (BPs, MFs, CCs) is presented in Table 2. The significant BPs are mainly enriched in the negative regulation of chemokine production, liver development and response to peptide, etc. The significant MFs enriched in the histone serine kinase activity, histone kinase activity, interleukin-6 receptor binding, etc. The significant CCs are enriched in the spindle microtubule, condensed chromosome, microtubule, etc. Different pathways; KEGG, WikiPathways, and BioCarta analysis results are presented in Table 3. The KEGG pathways for the hub genes are enriched in several pathways such as inflammatory bowel disease, AGE-RAGE signaling pathway in diabetic complications, pathways in cancer and coronavirus disease, etc. The WikiPathways pathway analysis results enhanced in Photodynamic therapy-induced NF-kB survival signaling WP3617, FOXP3 in COVID-19 WP5063, COVID-19 adverse outcome pathway WP4891, STING pathway in Kawasaki-like disease and COVID-19 WP4961, and Host-pathogen interaction of human coronaviruses—interferon induction WP4880, etc. BioCarta is mostly involved in Interleukin-27-mediated signaling events, FRA pathway, Interleukin-23-mediated signaling events and so on.

Hub-genes regulatory network analysis

We identified SRF, PBX1, MEIS1, ESR1 and MYC hub-TFs (Fig 4A), and hsa-miR-106b-5p, hsa-miR-20b-5p, hsa-miR-93-5p, hsa-miR-106a-5p and hsa-miR-20a-5p hub-miRNAs (Fig 4B) from the TFs-HubGs and miRNA-HubGs interaction network, respectively.

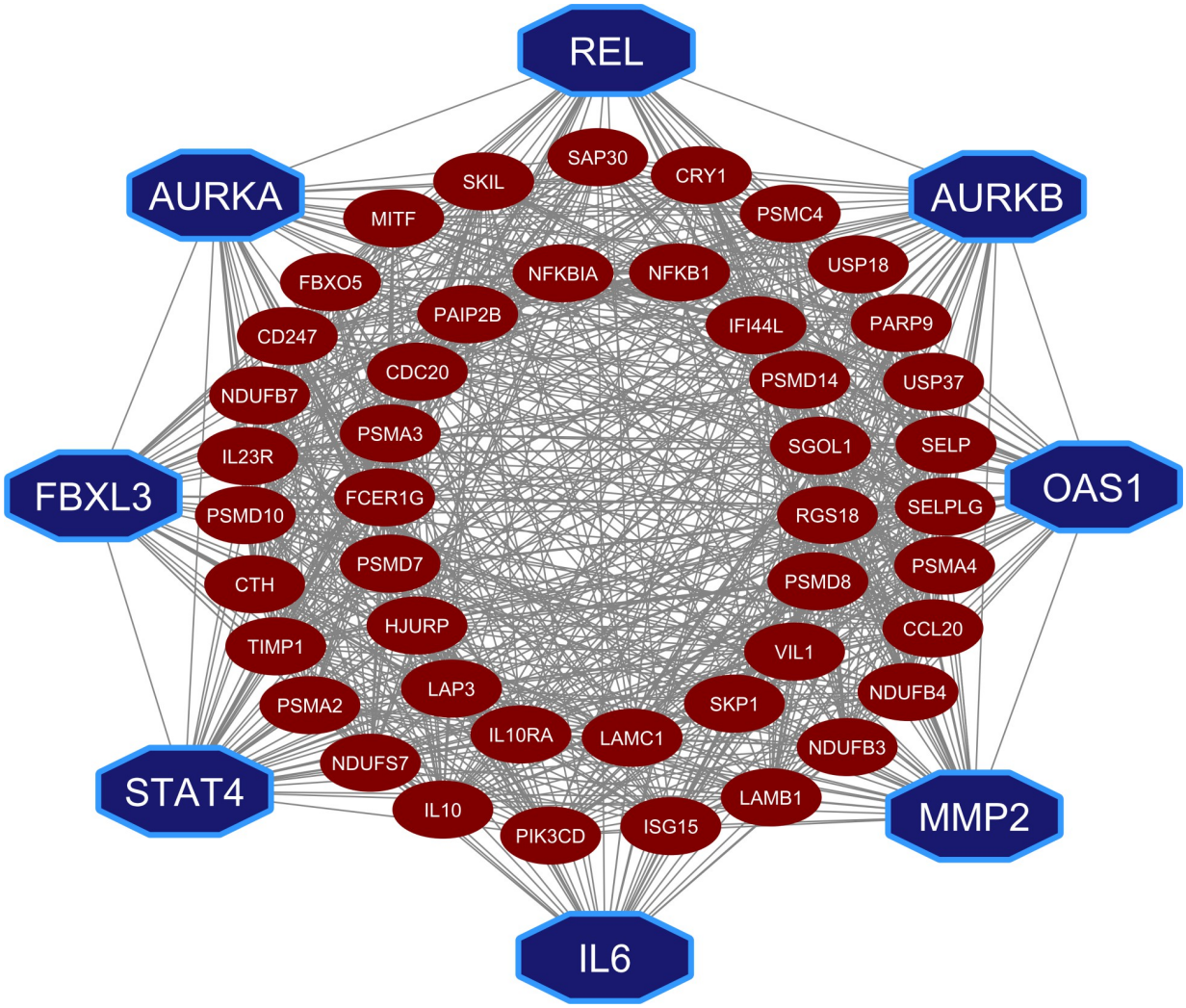

Fig 3. PPI network of validated DEGs to identify hub-genes.

https://doi.org/10.1371/journal.pone.0281981.g003

Exploring candidate drugs by molecular docking simulation

We considered HubGs mediated 8 proteins (REL, AURKA, AURKB, FBXL3, OAS1, STAT4, MMP2 and IL6) and their regulatory 5 hub-TFs proteins (SRF, PBX1, MEIS1, ESR1 and MYC) as the receptor proteins. The 3D structure of REL, AURKA, AURKB, FBXL3, OAS1, STAT4, MMP2, IL6, SRF, PBX1, MEIS1, ESR1 and MYC; targets were downloaded from PDB (Protein Data Bank) using the codes 1a3q, 6gra, 3af3, 4i6j, 4ig8, 4gj2, 3ayu, 5fuc, 1srs, 1puf, 5ego, 1uom, and 6e16, respectively. Then we considered 177 drug molecules (drug agents) that were selected by the literature review of COVID-19 related articles (S1 Table) and downloaded their 3D structures from the PubChem database. Then we performed molecular docking analysis of each receptor with each agent.

Fig 5A displayed the binding affinity score matrix between the ordered receptors and drug agents. We observed that each of the top 10 lead compounds (Nilotinib, Tegobuvir, Digoxin Proscillaridin, Olysio, Simeprevir, Hesperidin, Oleanolic Acid, Naltrindole and Danoprevir) produces binding affinity scores less than or equal to -7.0 kcal/mol with all of our suggested

Table 2. Significantly enriched top-ranked 6 GO-terms with hub-genes.

Category	GO-ID	GO-terms	P-values (Adjusted)	Hub-genes
Biological process (BP)	GO:0032682	negative regulation of chemokine production	<0.001	IL6, OAS1
	GO:0001889	liver development	<0.001	IL6, AURKA
	GO:1901652	response to peptide	<0.001	MMP2, STAT4
	GO:0060700	regulation of ribonuclease activity	0.003	OAS1
	GO:0061888	regulation of astrocyte activation	0.003	IL6
	GO:0032466	negative regulation of cytokinesis	0.003	AURKB
Molecular Function (MF)	GO:0035174	histone serine kinase activity	<0.001	AURKA, AURKB
	GO:0035173	histone kinase activity	<0.001	AURKA, AURKB
	GO:0005138	interleukin-6 receptor binding	0.009	IL6
	GO:0004674	protein serine/threonine kinase activity	0.018	AURKA, AURKB
	GO:0070566	adenylyltransferase activity	0.018	OAS1
	GO:0004222	metalloendopeptidase activity	0.041	MMP2
Cellular Component (CC)	GO:0005876	spindle microtubule	0.002	AURKA, AURKB
	GO:0005874	microtubule	0.007	AURKA, AURKB
	GO:0005819	spindle	0.007	AURKA, AURKB
	GO:0000779	condensed chromosome, centromeric region	0.009	AURKB
	GO:0015630	microtubule cytoskeleton	0.013	AURKA, AURKB
	GO:0043231	Intracellular membrane-bounded organelle	0.032	OAS1, REL, FBXL3, AURKA, AURKB

https://doi.org/10.1371/journal.pone.0281981.t002

Table 3. Significantly enriched top-ranked 6 biological pathways with hub-genes in different databases.

Databases	Pathways	P-values (Adjusted)	Hub-genes
KEGG	Inflammatory bowel disease	0.003	IL6, STAT4
	AGE-RAGE signaling pathway in diabetic complications	0.003	IL6, MMP2
	Pathways in cancer	0.003	IL6, MMP2, STAT4
	Measles	0.003	IL6, OAS1
	Influenza A	0.003	IL6, OAS1
	Coronavirus disease	0.004	IL6, OAS1
WikiPathways	Photodynamic therapy-induced NF-kB survival signaling WP3617	<0.001	IL6, MMP2, REL
	miRNAs involvement in the immune response in sepsis WP4329	<0.001	IL6, REL
	Interferon type I signaling pathways WP585	<0.001	REL, STAT4
	FOXP3 in COVID-19 WP5063	0.007	IL6
	COVID-19 adverse outcome pathway WP4891	0.007	IL6
	STING pathway in Kawasaki-like disease and COVID-19 WP4961	0.009	REL
	Host-pathogen interaction of human coronaviruses—interferon induction WP4880	0.013	OAS1
BioCarta	Interleukin-27-mediated signaling events	<0.001	IL6, STAT4
	FRA pathway	<0.001	IL6, MMP2
	Interleukin-23-mediated signaling events	<0.001	IL6, STAT4
	Aurora B signaling	<0.001	AURKB, AURKA
	Alpha-M beta-2 integrin signaling	<0.001	IL6, MMP2
	FOXM1 transcription factor network	<0.001	MMP2, AURKB

https://doi.org/10.1371/journal.pone.0281981.t003

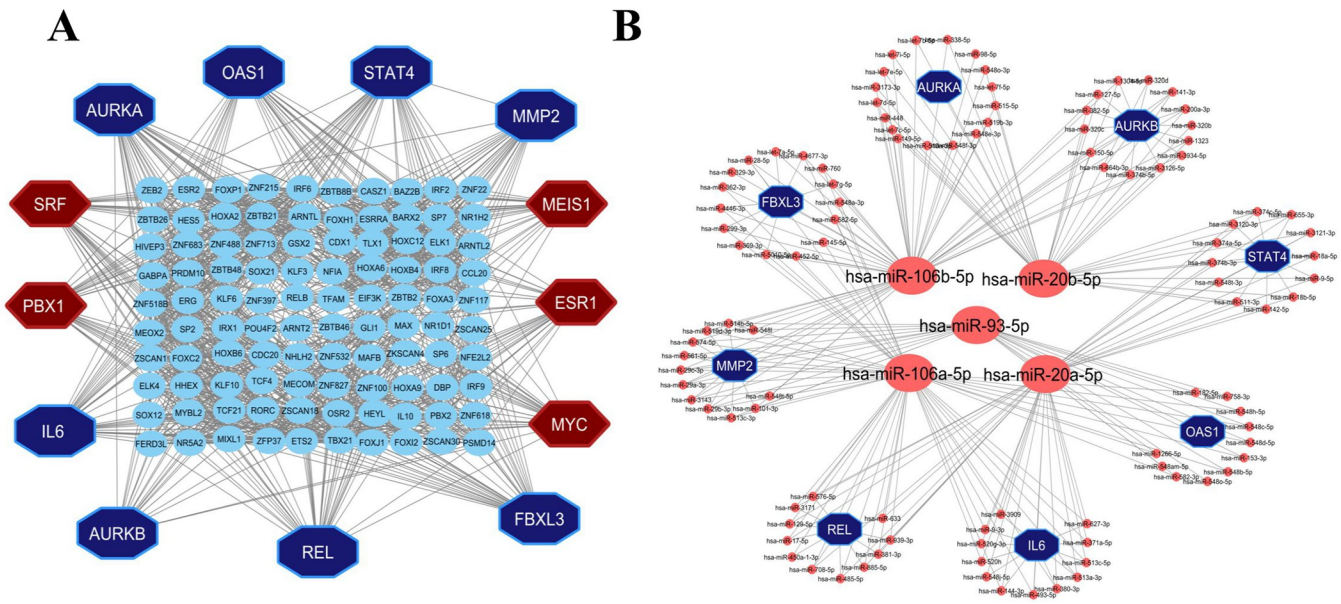

Fig 4. Hub-genes regulatory network analysis with (A) Transcription factors (TFs) and (B) micro RNAs (miRNAs).

https://doi.org/10.1371/journal.pone.0281981.g004

receptors (Section-I in S1 File for score matrix). Therefore, we considered these 10 drugs as the candidate drug agents in this study. To validate the proposed drugs against the state-of-the-art alternative independent receptors, we considered the top-ranked 8 hub-genes (*CASP3*, *CXCL8*, *ICAM1*, *IL6*, *NFKBIA*, *STAT1*, *TNF* and *IRF7*) that are common in at least 3 articles (S2 Table) out of 24. The 3D structures of these 8 independent receptor proteins were downloaded from Protein Data Bank (PDB) with codes 4ps0, 6n2u, 5mza, 5fuc, 1nfi, 1bf5, and 7kba, and receptor protein IRF7 were retrieved from the SWISS-MODEL using the UniProt IDs Q92985, respectively. Fig 5B represents the binding affinities (kcal/mol) between the proposed drugs and publicly available top-ranked independent receptors. We observed that three lead compounds (lead1: Tegobuvir, lead2: Nilotinib, lead3: Proscillaridin) strongly bind with all independent receptors (Section-II in S1 File for score matrix). Table 4 represents the summary results of interacting properties of the top targets with top-ranked lead compounds that produced highest binding scores. We also examined their complete interaction profile including hydrophobic, hydrogen bonds, and electrostatic interactions. We illustrated 2D structure of proteins and ligands interaction in Fig 6. The 3D structure of their interacting complex and top-ranked lead compounds are shown in the Fig 7. To investigate the stability of the top three complexes, we performed molecular dynamic simulations as discussed in the next section.

Molecular Dynamic (MD) simulations

Three predicted drug agents (Nilotinib, Tegobuvir, and Proscillaridin) showed the highest binding affinities with AURKA, AURKB, and OAS1 proteins, respectively (Table 4). Therefore, three complexes (AURKA *vs*. Nilotinib, AURKB *vs*. Tegobuvir, and OAS1 *vs*. Proscillaridin) were considered for stability analysis using 100 ns MD-based MM-PBSA simulations. We observed that these 3 complexes (AURKA *vs*. Nilotinib, AURKB vs Tegobuvir, OAS1 *vs*. Proscillaridin) showed significant stability between the variations of moving and initial drug-target protein complexes (Fig 8A). RMSD values corresponding to each complex were calculated. All the systems projected the RMSD values around 1.5 Å to 4.15 Å. The average RMSD values for AURKA *vs*. Nilotinib, AURKB *vs*. Tegobuvir, and OAS1 *vs*. Proscillaridin complexes were

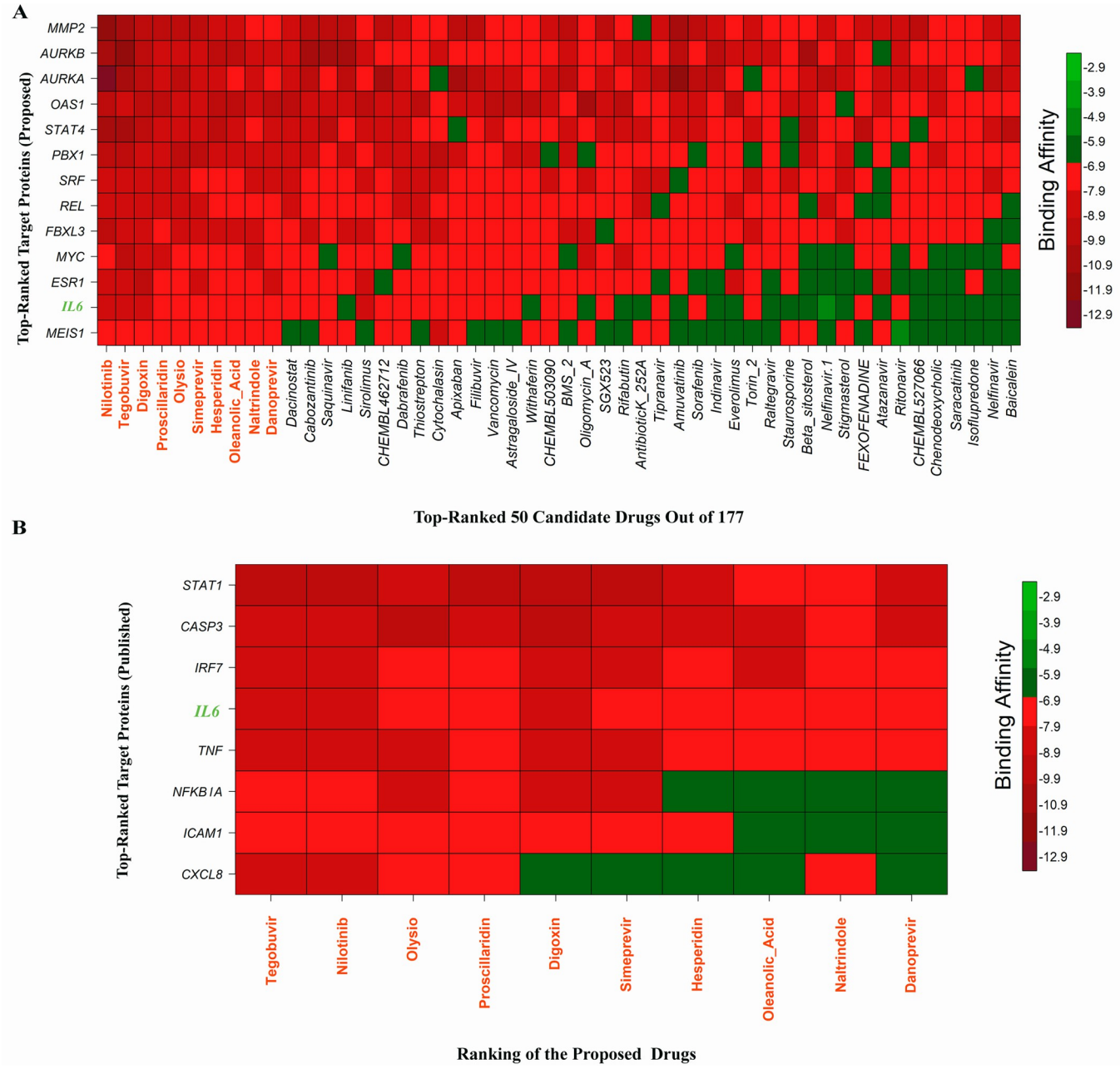

Fig 5. Matrix of binding affinity scores between receptors and ligands computed by molecular docking. (A) Row indicates ordered 13 proposed receptor proteins and column indicates the top-ordered 50 drug agents out of 158, where red colors indicate the strong binding affinities, (B) Row indicates top-ranked 8 receptor proteins obtained through published literature, and column indicates the proposed top-ordered 10 drug agents out of 158, where red colors indicate the strong binding affinities.

https://doi.org/10.1371/journal.pone.0281981.g005

2.543 Å, 2.863 Å, and 2.324 Å, respectively. The OAS1 *vs*. Proscillaridin complex displayed a more rigid conformation than the other complexes, reached equilibrium at 35 ns, and remained almost stable, after that AURKA *vs*. Nilotinib complex showed almost stable performance during 10 ns to 35 ns, 52 ns to 70 ns and the remaining times there were irregular fluctuations in the RMSD. On the contrary, AURKB *vs*. Tegobuvir complexes exhibited irregular fluctuation and RMSD values fluctuate from 2.0 Å to 4.15 Å over the time period. In addition,

Table 4. Docking results of interacting proteins and drugs. The last row shows key interactions of amino acids and their binding types with potential targets.

Potential Targets		AURKA	AURKB	OAS1
Potential Ligands		Nilotinib	Tegobuvir	Proscillaridin
Binding Affinity (kcal/ mol)		-12	-11	-9.8
Interacting Amino Acids	Hydrogen Bond	LYS143	LEU83, GLU161	SER63, ASN307, GLN 194, GLY306
	Hydrophobic Interactions	LEU169, LEU263, LEU164, ALA273, ALA213, LYS143, VAL147, ALA160, LEU194, GLU211, LEU139, GLU260, GLY140, LYS162, ASN261, GLU181, LEU208, LEU178, GLN177, VAL174	GLU204, LYS106, PYS106, PHE219, LEU207, ALA217, VAL91, LEU154, PHE88, LEU83,	PRO228, LEU308, TYR230, ASP300, THR188, ASP77, LEU308, LEU150, SER187, GLY184, GLY306, GLY311, GLY310, GLN 183
	Electrostatic	LYS143	-	-

https://doi.org/10.1371/journal.pone.0281981.t004

MM-PBSA binding energy for three complexes were also calculated, and Fig 8B illustrated the binding energies of the complexes. On average, AURKA *vs*. Nilotinib, AURKB *vs*. Tegobuvir, and OAS1 *vs*. Proscillaridin complexes produced MM-PBSA binding energies 58.5 kcal/mol, 53.92 kcal /mol, and– 6.834 kcal /mol, respectively.

Discussion

COVID-19 is the most recent and ongoing pandemic that has adversely affected on human health and the world's economy. Though vaccination programs were started globally at a marginal rate, it is still a threat to public health. Gene signatures are the pathological indicator for describing diseases at a molecular level. In this study, we used bioinformatics approach to detect gene signatures and potential therapeutic drugs for the treatment of COVID-19 patients. The present study employed three different datasets (Table 1) to identify potential DEGs between COVID-19 and control samples. The results of the analysis revealed a total of 2389 and 540 DEGs from two RNA-Seq datasets and 2102 DEGs from the microarray dataset. To select the potential DEGs, we validated these 3 DEGs-sets by WGCNA, PA and RRA procedures. Then we selected top-ranked 50 DEGs as the most potential DEGs. We performed protein-protein interaction (PPI) network analysis of those 50 DEGs to select the HubGs. Finally, we selected top-ranked 8 DEGs (*REL*, *AURKA*, *AURKB*, *FBXL3*, *OAS1*, *STAT4*, *MMP2*, *IL6*) as the HubGs (Fig 3), that were used for further investigation of SARS-CoV-2 infections. The literature review also supported these HubGs as the SARS-CoV-2 infection-causing genes (Fig 9A). As for example, the gene *REL* has been previously reported as a hub gene for SARS-CoV-2 infections [16]. By combining some studies, we found that the gene *AURKA* is a common targeted protein for both COVID-19 and lung adenocarcinoma patients [14,17,62]. The gene *AURKB* plays a crucial role as a biomarker gene in the diagnosis and prognosis of COVID-19 patients [14]. The gene *FBXL3* has been identified as a core gene of COVID-19 [14,63–65]. It has been noted that the gene *OAS1* is an important gene influencing COVID-19 patients [66–70]. The gene *STAT4* is the human transcriptomic factor of COVID-19 [71–73]. The gene *MMP2* has been recognized as a hub gene in COVID-19-infected patients [13,74]. The gene *IL-6* can safeguard against basic circumstances with coronavirus, diminishing IL-6 articulation [75–83]. The interaction network analysis between HubGs and transcription factors (TFs) revealed the top-ranked 5 TFs genes (SRF, PBX1, MEIS1, ESR1 and MYC*)* as the key transcriptional regulators of HubGs (Fig 4A). Notably, the SRF gene demonstrated a unique and dysfunctional pattern in COVID-19 [5,6,84,85]. The TF genes PBX1 has been found to possess multiple functions relevant to cell development and has been associated with tumor agents and COVID-19 [16,86], MEIS1 has been identified as the targeted agent of SARS-CoV-2 [16,87], ESR1 has been noted to act as an antiviral signature that disrupts the

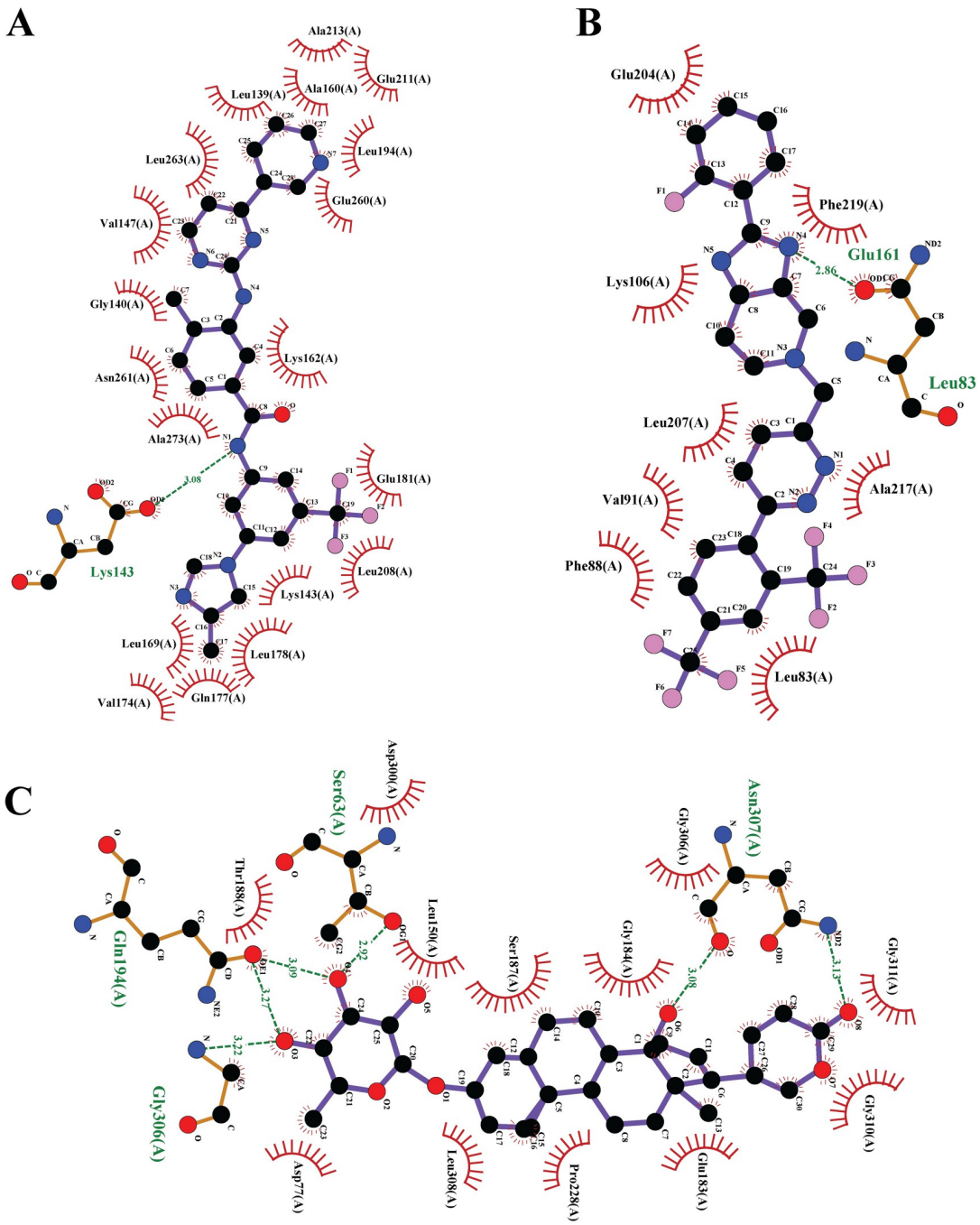

Fig 6. The 2D view of strong binding interactions between targets and drugs are shown by Ligplot. (A) AURKA *vs*. Nilotinib, (B) AURKB *vs*. Tegobuvir, and (C) OAS1 *vs*. Proscillaridin.

https://doi.org/10.1371/journal.pone.0281981.g006

viral membrane of the SARS-CoV-2 protein [88]. Furthermore, MYC is another target gene of COVID-19, has been reported to have various functions, including regulation of chromatin sites, modulation of cellular metabolism, and versatility across various cell types [87,88]. The hub-genes versus micro-RNA interaction network analysis revealed top-ranked 5 miRNAs (hsa-miR-106b-5p, hsa-miR-20b-5p, hsa-miR-93-5p, hsa-miR-106a-5p and hsa-miR-20a-5p) as the post-transcriptional regulators of hub-genes (Fig 4B). The miRNA, hsa-miR-106b-5p,

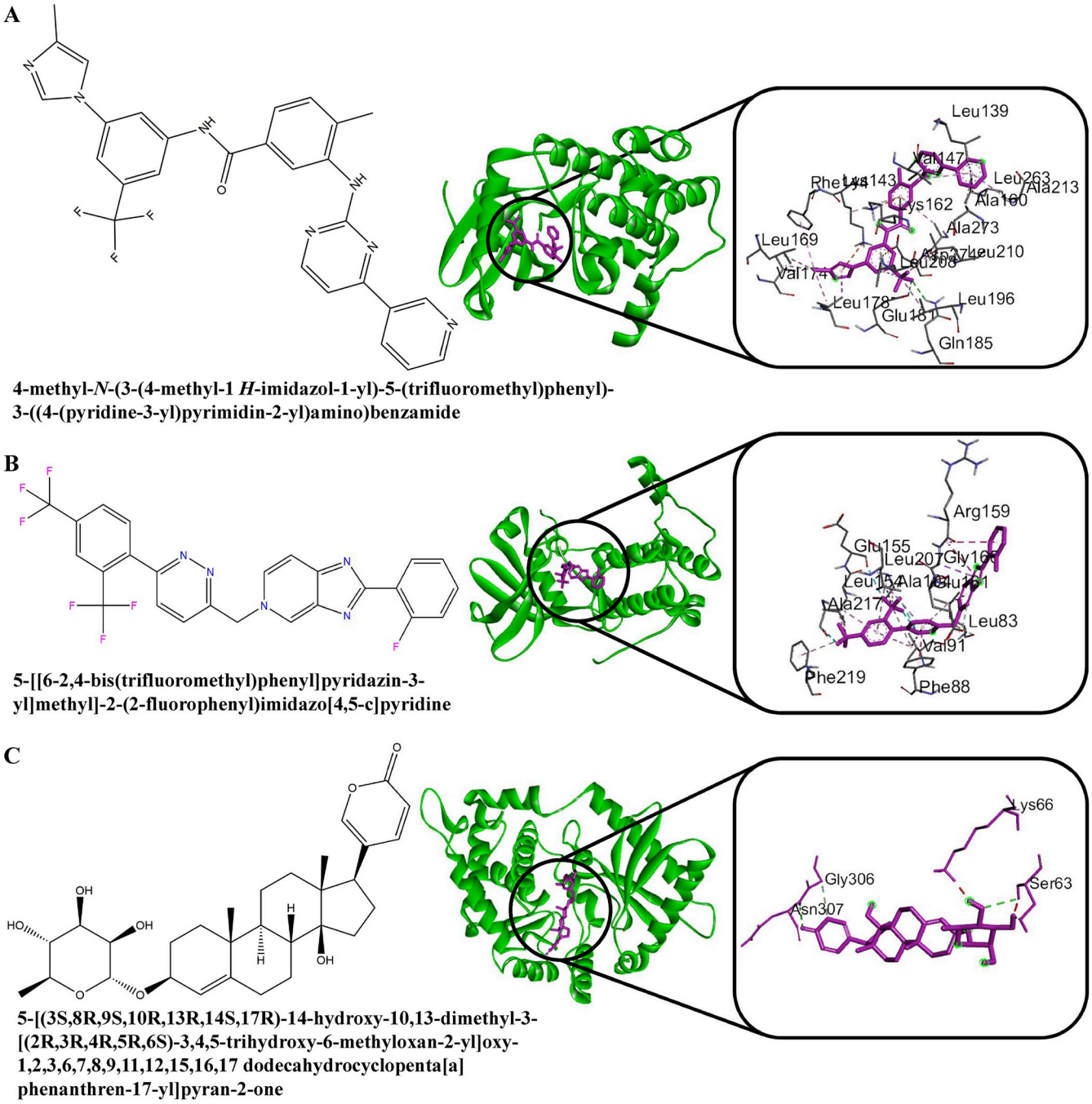

Fig 7. Lead compound (left side) and three complexes of three-dimensional chemical interactions (right side) obtained from molecular docking. (a) AURKA *vs*. Nilotinib, (b) AURKB *vs*. Tegobuvir, and (c) OAS1 *vs*. Proscillaridin.

https://doi.org/10.1371/journal.pone.0281981.g007

has been identified as a tumor promoter and targeted receptor for different cancers [89]. The hsa-miR-20b-5p miRNA has been shown to play an antiviral role in patients infected with SARS-CoV and SARS-CoV-2, as well as the up-regulated signature of the influenza virus [90]. The hsa-miR-93-5p miRNA is associated with human cancerous growth and encourages angiogenic operation [91]. The miRNA, hsa-miR-106a-5p, promotes virus mechanism of

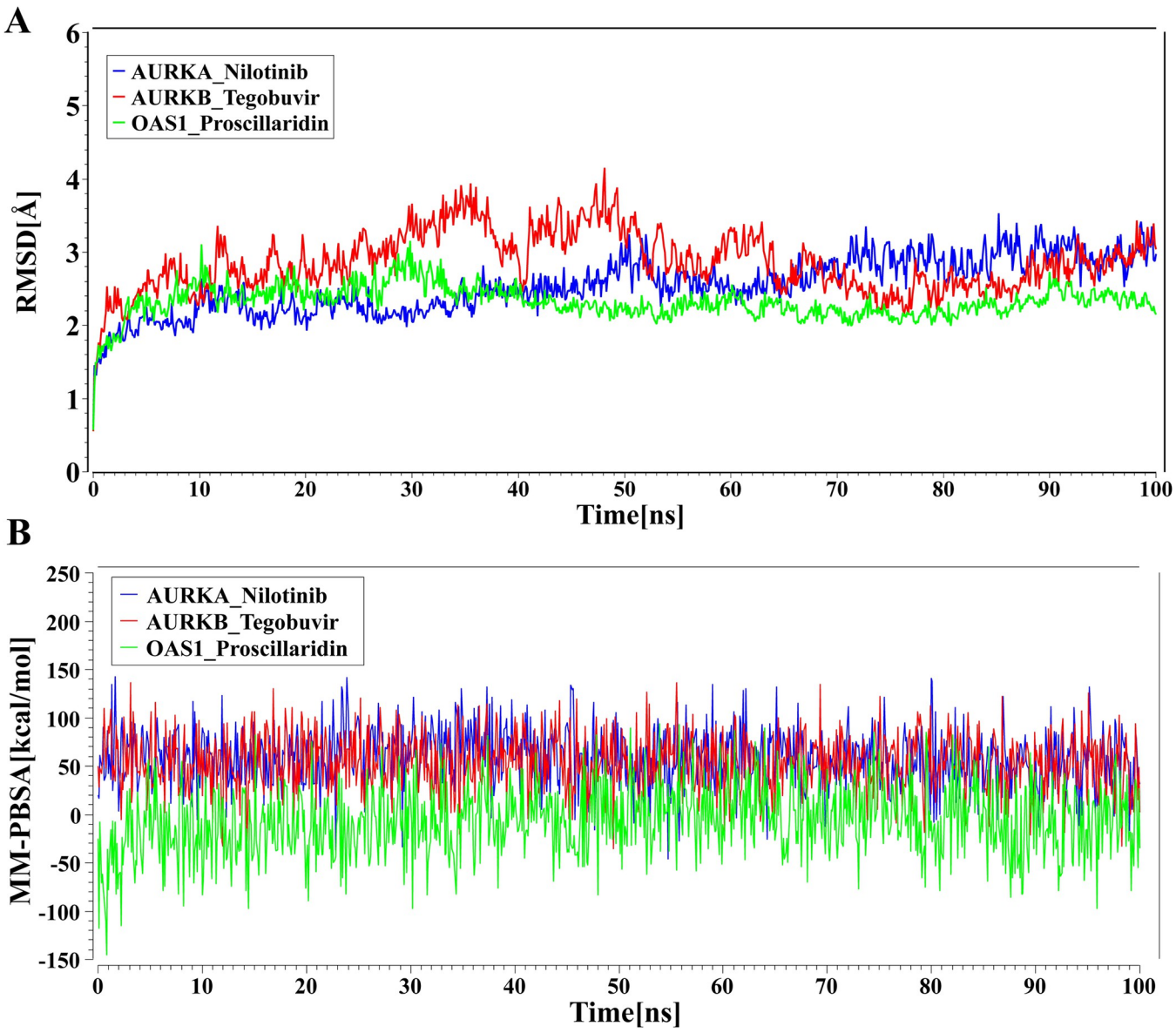

Fig 8. MD simulations of top-ranked three complexes. (A) Time evolution of RMSDs for each of the top-ranked three complexes. (B) Binding free energy (kcal/mol) of each snapshot was calculated by MM-PBSA, representing the change in binding stability of each complex during simulations; positive values indicate better binding. Complexes: blue AURKA *vs*. Nilotinib, red AURKB *vs*. Tegobuvir, and green. OAS1 *vs*. Proscillaridin.

https://doi.org/10.1371/journal.pone.0281981.g008

COVID-19 [92]. The miRNA, hsa-miR-20a-5p has been shown to play a significant role in respiratory viruses including adenovirus 2, influenza A and RSV [93].

To explore the biological insights underlying HubGs we used web-based tool *Enrichr*. Pathological information of HubGs described the significance of biomarker agents by using gene ontology and pathway analysis. GO analysis enriched with the regulation of acute inflammatory response [11], interleukin-6 receptor binding [94], and Intracellular membrane-bounded organelle [95] (Table 2). KEGG pathway associated with influenza A, coronavirus disease [96], bladder cancer and malaria. WikiPathways Interferon type I signaling pathways WP585, FOXP3 in COVID-19 WP5063, COVID-19 adverse outcome pathway WP4891, STING pathway in Kawasaki-like disease and COVID-19 WP4961 (Table 3). To find the effective drug

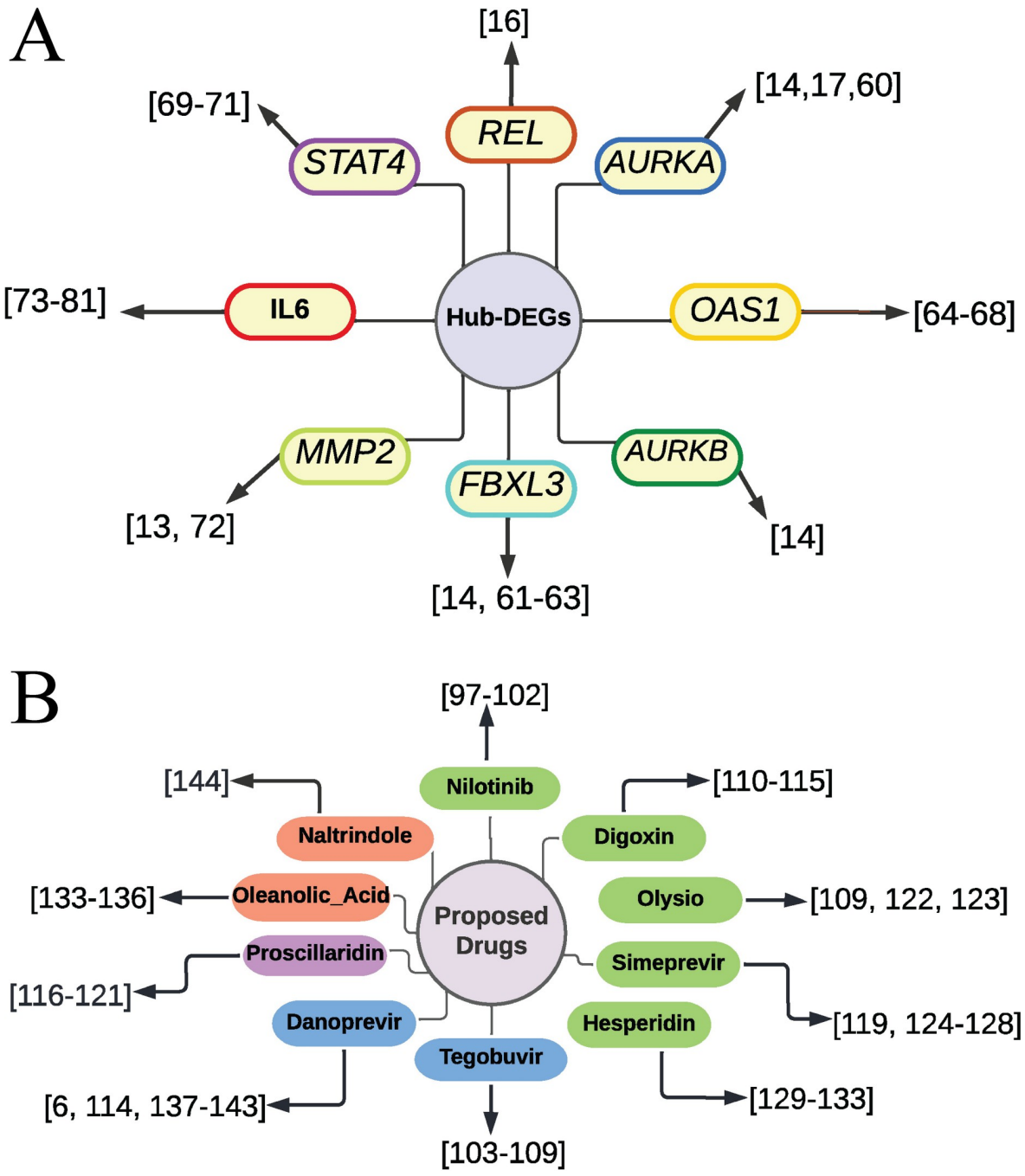

Fig 9. Validation of hub genes and candidate drugs in favor of SARS-CoV-2 by the literature review. (A) Validation of the proposed HubGs: circles with node color indicates hub genes, and each connected network with number(s) indicates the reference(s) of gene(s) of SARS-CoV-2 (B) Validation of the proposed candidate drugs: circles with green color indicate FDA approved, light blue color indicates investigational drugs and purple color indicates experimental drugs and red color indicates unapproved drugs, and each connected network with number(s) indicates the reference(s) of drug(s) of SARS-CoV-2.

https://doi.org/10.1371/journal.pone.0281981.g009

molecules against COVID-19, we used the proposed 8 target proteins and their regulatory 5 key TFs proteins as the receptor proteins. We performed their docking analysis with 177 meta-drug agents (S1 File).

Then we picked up the top-ranked 10 drugs (Nilotinib, Tegobuvir, Digoxin, Proscillaridin, Olysio, Simeprevir, Hesperidin, Oleanolic Acid, Naltrindole, and Danoprevir) as the candidate drug agents based on their strong binding affinities with all the target proteins (Fig 5A). These drug molecules are also supported by other individual studies for the treatment against SARS-CoV-2 infections which includes Nilotinib [97–102], Tegobuvir [103–109], Digoxin [110–115], Proscillaridin [116–121], Olysio [109,122,123], Simeprevir [119,124–128], Hesperidin [129–133], Oleanolic Acid [133–136], Danoprevir [6,114,137–143], Naltrindole [144] for the treatment against COVID-19 (Fig 9B). Fig 5B displays the results of cross-validation of our suggested ten candidate drug agents with the top-ranked independent receptor proteins, and observed their strong binding affinities. Finally, the binding stability of the top three complexes (AURKA vs. Nilotinib, AURKB vs. Tegobuvir, and OAS1 vs. Proscillaridin) were investigated by molecular dynamics (MD) based MM-PBSA simulations, which revealed their stable performance (Fig 8) [145,146].

The phylogenetic tree and pairwise alignment results on identities, similarities and gaps of HubGs (*REL*, *AURKA*, *AURKB*, *FBXL3*, *OAS1*, *STAT4*, *MMP2* and *IL6*) protein sequences showed that AURKA and AURKB proteins are more-closer to each other with largest identity (54.3%) and similarity (63.4%) and, smallest gap (28.3%) compares to any other pair of HubGs (S2 File for MSA, phylogenetic tree, identity, similarity, score and gaps). The binding affinity scores of these two proteins were found significantly larger and almost same with respect to our suggested drug molecules (Fig 5A). On the other hand, we also observed that proteins OAS1 and FBXL3 are second more-closer to each other with larger identity (28.7%) and similarity (37.0%) and, smaller gap (52.7%) compares to any other pair of the rest HubGs. The binding affinity scores for these two proteins were also larger and almost similar against our suggested drug molecules. The MD simulation-based MM-PBSA analysis showed the average binding free energy for AURKA and AURKB are almost similar (58.5 kcal/mol & 53.92 kcal/mol) but far different from OAS1 (-6.834 kcal/mol). Thus, the molecular signatures and potential repurposable drug agents that we have identified in this study may serve as valuable resources for wet-lab validation and the development of an effective treatment plan against SARS-CoV-2 infections.

Conclusions

This study suggested SARS-CoV-2 infection causing core genes (*REL*, *AURKA*, *AURKB*, *FBXL3*, *OAS1*, *STAT4*, *MMP2* and *IL6*) by highlighting their key transcriptional regulators (SRF, PBX1, MEIS1, ESR1 and MYC) and post-transcriptional regulators (hsa-miR-106b-5p, hsa-miR-20b-5p, hsa-miR-93-5p, hsa-miR-106a-5p and hsa-miR-20a-5p). To explore the effective drugs for SARS-CoV-2 infections by the molecular docking analysis, core gene mediated proteins and five TFs proteins were considered as the receptors. Based on our computational analysis, we nominated top-ranked 10 candidate drugs (Nilotinib, Tegobuvir, Digoxin, Proscillaridin, Olysio, Simeprevir, Hesperidin, Oleanolic Acid, Naltrindole, and Danoprevir) that showed the highest docking scores, indicating their favorable binding affinity with the receptors. Then we validated the suggested drug molecules against the state-of-the-art alternatives publicly available top-ranked 8 independent receptors (CASP3, CXCL8, ICAM1, IL6, NFKBIA, STAT1, TNF and IRF7) by molecular docking and found their significant binding affinities. Finally, we examined the stability of top-ranked three receptor-ligand complexes (AURKA vs. Nilotinib, AURKB vs. Tegobuvir, OAS1 vs. Proscillaridin) by computing the RMSD scores and binding free energies through the 100 ns MD-simulation based MM-PBSA approach, and observed their stable performance. In this regard, this study might open up a new gateway to explore more effective drug molecules computationally against SARS-CoV-2

infections. Thus, the outputs of this study might be useful inputs for wet-lab experiment to make a proper treatment plan against SARS-CoV-2 infections.

Supporting information

S1 Table. Collection of 177 meta drug agents by literature review.
(DOCX)

S2 Table. Targeted protein list from different published literature.
(DOCX)

S1 File. (I) Binding score of the interaction of targeted proteins with targeted drugs. (II) Binding score of the interaction of published proteins with proposed drugs and published drugs.
(XLSX)

S2 File. (I) Multiple Sequence Alignment (MSA) Results for HubGs. (II) Identity, Similarity, Gap and Score matrices based on the alignment results of HubGs. (III) Phylogenetic tree of HubGs.
(XLSX)

Acknowledgments

We are thankful to the reviewers for his/her help in improving the quality of the manuscript.

Author Contributions

Conceptualization: Bandhan Sarker, Md. Matiur Rahaman, Md. Nurul Haque Mollah.

Data curation: Bandhan Sarker, Md. Ariful Islam.

Formal analysis: Bandhan Sarker, Md. Ariful Islam.

Methodology: Md. Matiur Rahaman, Md. Maidul Husain, Md. Asif Ahsan.

Supervision: Md. Matiur Rahaman, Md. Nurul Haque Mollah.

Validation: Muhammad Habibulla Alamin, Farzana Ferdousi, Md. Nurul Haque Mollah.

Visualization: Bandhan Sarker, Md. Ariful Islam, Muhammad Habibulla Alamin, Md. Nurul Haque Mollah.

Writing – original draft: Bandhan Sarker, Md. Matiur Rahaman, Md. Ariful Islam.

Writing – review & editing: Md. Matiur Rahaman, Muhammad Habibulla Alamin, Md. Maidul Husain, Farzana Ferdousi, Md. Asif Ahsan, Md. Nurul Haque Mollah.

References

1. Cucinotta D, Vanelli M. WHO declares COVID-19 a pandemic. Acta Bio Medica: Atenei Parmensis. 2020; 91: 157. https://doi.org/10.23750/abm.v91i1.9397 PMID: 32191675
2. Chen N, Zhou M, Dong X, Qu J, Gong F, Han Y, et al. Epidemiological and clinical characteristics of 99 cases of 2019 novel coronavirus pneumonia in Wuhan, China: a descriptive study. The lancet. 2020; 395: 507–513. https://doi.org/10.1016/S0140-6736(20)30211-7 PMID: 32007143
3. Cao B, Wang Y, Wen D, Liu W, Wang J, Fan G, et al. A trial of lopinavir–ritonavir in adults hospitalized with severe Covid-19. New England Journal of Medicine. 2020.
4. Zhou P, Yang X-L, Wang X-G, Hu B, Zhang L, Zhang W, et al. A pneumonia outbreak associated with a new coronavirus of probable bat origin. nature. 2020; 579: 270–273. https://doi.org/10.1038/s41586-020-2012-7 PMID: 32015507

5. Mosharaf MdP Reza MdS, Kibria MdK Ahmed FF, Kabir MdH Hasan S, et al. Computational identification of host genomic biomarkers highlighting their functions, pathways and regulators that influence SARS-CoV-2 infections and drug repurposing. Sci Rep. 2022; 12: 4279. https://doi.org/10.1038/s41598-022-08073-8 PMID: 35277538

6. Ahmed FF, Reza MdS, Sarker MdS, Islam MdS, Mosharaf MdP, Hasan S, et al. Identification of host transcriptome-guided repurposable drugs for SARS-CoV-1 infections and their validation with SARS-CoV-2 infections by using the integrated bioinformatics approaches. Ashfaq UA, editor. PLoS ONE. 2022; 17: e0266124. https://doi.org/10.1371/journal.pone.0266124 PMID: 35390032

7. D'Orazio M, Bernardini G, Quagliarini E. A probabilistic model to evaluate the effectiveness of main solutions to COVID-19 spreading in university buildings according to proximity and time-based consolidated criteria. Building simulation. Springer; 2021. pp. 1795–1809.

8. Kitchin R. Civil liberties or public health, or civil liberties and public health? Using surveillance technologies to tackle the spread of COVID-19. Space and Polity. 2020; 24: 362–381.

9. Mohammadpour S, Torshizi Esfahani A, Halaji M, Lak M, Ranjbar R. An updated review of the association of host genetic factors with susceptibility and resistance to COVID-19. Journal of Cellular Physiology. 2021; 236: 49–54. https://doi.org/10.1002/jcp.29868 PMID: 32542735

10. Zhang X, Tan Y, Ling Y, Lu G, Liu F, Yi Z, et al. Viral and host factors related to the clinical outcome of COVID-19. Nature. 2020; 583: 437–440. https://doi.org/10.1038/s41586-020-2355-0 PMID: 32434211

11. Tay MZ, Poh CM, Rénia L, MacAry PA, Ng LF. The trinity of COVID-19: immunity, inflammation and intervention. Nature Reviews Immunology. 2020; 20: 363–374. https://doi.org/10.1038/s41577-020-0311-8 PMID: 32346093

12. Yuan D, Zhou H, Sun H, Tian R, Xia M, Sun L, et al. Identification of key genes for guiding chemotherapeutic management in ovarian cancer using translational bioinformatics. Oncology letters. 2020; 20: 1345–1359. https://doi.org/10.3892/ol.2020.11672 PMID: 32724377

13. Nan KS, Karuppanan K, Kumar S. Identification of common key genes and pathways between Covid-19 and lung cancer by using protein-protein interaction network analysis. Bioinformatics; 2021 Feb. https://doi.org/10.1101/2021.02.16.431364

14. Auwul MR, Rahman MR, Gov E, Shahjaman M, Moni MA. Bioinformatics and machine learning approach identifies potential drug targets and pathways in COVID-19. Briefings in Bioinformatics. 2021; 22: bbab120. https://doi.org/10.1093/bib/bbab120 PMID: 33839760

15. Karami H, Derakhshani A, Ghasemigol M, Fereidouni M, Miri-Moghaddam E, Baradaran B, et al. Weighted Gene Co-Expression Network Analysis Combined with Machine Learning Validation to Identify Key Modules and Hub Genes Associated with SARS-CoV-2 Infection. Journal of clinical medicine. 2021; 10: 3567. https://doi.org/10.3390/jcm10163567 PMID: 34441862

16. Vastrad B, Vastrad C, Tengli A. Bioinformatics analyses of significant genes, related pathways, and candidate diagnostic biomarkers and molecular targets in SARS-CoV-2/COVID-19. Gene Reports. 2020; 21: 100956. https://doi.org/10.1016/j.genrep.2020.100956 PMID: 33553808

17. Reza MdS Harun-Or-Roshid Md, Islam MdA Hossen MdA, Hossain MdT, Feng S, et al. Bioinformatics Screening of Potential Biomarkers from mRNA Expression Profiles to Discover Drug Targets and Agents for Cervical Cancer. IJMS. 2022; 23: 3968. https://doi.org/10.3390/ijms23073968 PMID: 35409328

18. Alam MS, Rahaman MM, Sultana A, Wang G, Mollah MNH. Statistics and network-based approaches to identify molecular mechanisms that drive the progression of breast cancer. Computers in Biology and Medicine. 2022; 145: 105508. https://doi.org/10.1016/j.compbiomed.2022.105508 PMID: 35447458

19. Liu R, Zhang W, Liu Z-Q, Zhou H-H. Associating transcriptional modules with colon cancer survival through weighted gene co-expression network analysis. BMC genomics. 2017; 18: 1–9.

20. Jin X, Li J, Li W, Wang X, Du C, Geng Z, et al. Weighted gene co-expression network analysis reveals specific modules and biomarkers in Parkinson's disease. Neuroscience Letters. 2020; 728: 134950. https://doi.org/10.1016/j.neulet.2020.134950 PMID: 32276105

21. Malik M, Parikh I, Vasquez JB, Smith C, Tai L, Bu G, et al. Genetics ignite focus on microglial inflammation in Alzheimer's disease. Molecular neurodegeneration. 2015; 10: 1–12.

22. Arunachalam PS, Wimmers F, Mok CKP, Perera RAPM, Scott M, Hagan T, et al. Systems biological assessment of immunity to mild versus severe COVID-19 infection in humans. Science. 2020; 369: 1210–1220. https://doi.org/10.1126/science.abc6261 PMID: 32788292

23. Blanco-Melo D, Nilsson-Payant BE, Liu W-C, Uhl S, Hoagland D, Møller R, et al. Imbalanced Host Response to SARS-CoV-2 Drives Development of COVID-19. Cell. 2020; 181: 1036–1045.e9. https://doi.org/10.1016/j.cell.2020.04.026 PMID: 32416070

24. Lieberman NA, Peddu V, Xie H, Shrestha L, Huang M-L, Mears MC, et al. In vivo antiviral host transcriptional response to SARS-CoV-2 by viral load, sex, and age. PLoS biology. 2020; 18: e3000849. https://doi.org/10.1371/journal.pbio.3000849 PMID: 32898168

25. Li Y, Jiang Y, Zhang Y, Li N, Yin Q, Liu L, et al. Abnormal upregulation of cardiovascular disease biomarker PLA2G7 induced by proinflammatory macrophages in COVID-19 patients. Scientific reports. 2021; 11: 1–11.

26. Liu J, Yuan S, Yao Y, Wang J, Scalabrino G, Jiang S, et al. Network Pharmacology and Molecular Docking Elucidate the Underlying Pharmacological Mechanisms of the Herb Houttuynia cordata in Treating Pneumonia Caused by SARS-CoV-2. Viruses. 2022; 14: 1588. https://doi.org/10.3390/v14071588 PMID: 35891565

27. Leek JT, Johnson WE, Parker HS, Jaffe AE, Storey JD. The sva package for removing batch effects and other unwanted variation in high-throughput experiments. Bioinformatics. 2012; 28: 882–883. https://doi.org/10.1093/bioinformatics/bts034 PMID: 22257669

28. Davis S, Meltzer PS. GEOquery: a bridge between the Gene Expression Omnibus (GEO) and BioConductor. Bioinformatics. 2007; 23: 1846–1847. https://doi.org/10.1093/bioinformatics/btm254 PMID: 17496320

29. Smyth GK, Ritchie M, Thorne N, Wettenhall J. LIMMA: linear models for microarray data. In Bioinformatics and Computational Biology Solutions Using R and Bioconductor. Statistics for Biology and Health. 2005.

30. Langfelder P, Horvath S. WGCNA: an R package for weighted correlation network analysis. BMC bioinformatics. 2008; 9: 1–13.

31. Langfelder P, Luo R, Oldham MC, Horvath S. Is my network module preserved and reproducible? PLoS computational biology. 2011; 7: e1001057. https://doi.org/10.1371/journal.pcbi.1001057 PMID: 21283776

32. Szklarczyk D, Franceschini A, Wyder S, Forslund K, Heller D, Huerta-Cepas J, et al. STRING v10: protein–protein interaction networks, integrated over the tree of life. Nucleic acids research. 2015; 43: D447–D452. https://doi.org/10.1093/nar/gku1003 PMID: 25352553

33. Saito R, Smoot ME, Ono K, Ruscheinski J, Wang P-L, Lotia S, et al. A travel guide to Cytoscape plugins. Nature methods. 2012; 9: 1069. https://doi.org/10.1038/nmeth.2212 PMID: 23132118

34. Kuleshov MV, Jones MR, Rouillard AD, Fernandez NF, Duan Q, Wang Z, et al. Enrichr: a comprehensive gene set enrichment analysis web server 2016 update. Nucleic acids research. 2016; 44: W90–W97. https://doi.org/10.1093/nar/gkw377 PMID: 27141961

35. Pujato M, Kieken F, Skiles AA, Tapinos N, Fiser A. Prediction of DNA binding motifs from 3D models of transcription factors; identifying TLX3 regulated genes. Nucleic acids research. 2014; 42: 13500–13512. https://doi.org/10.1093/nar/gku1228 PMID: 25428367

36. Wong N, Wang X. miRDB: an online resource for microRNA target prediction and functional annotations. Nucleic acids research. 2015; 43: D146–D152. https://doi.org/10.1093/nar/gku1104 PMID: 25378301

37. Berman HM, Battistuz T, Bhat TN, Bluhm WF, Bourne PE, Burkhardt K, et al. The Protein Data Bank. Acta Crystallogr D Biol Crystallogr. 2002; 58: 899–907. https://doi.org/10.1107/s0907444902003451 PMID: 12037327

38. Waterhouse A, Bertoni M, Bienert S, Studer G, Tauriello G, Gumienny R, et al. SWISS-MODEL: Homology modelling of protein structures and complexes. Nucleic Acids Research. 2018; 46. https://doi.org/10.1093/nar/gky427 PMID: 29788355

39. Kim S, Chen J, Cheng T, Gindulyte A, He J, He S, et al. PubChem 2019 update: Improved access to chemical data. Nucleic Acids Research. 2019; 47. https://doi.org/10.1093/nar/gky1033 PMID: 30371825

40. Visualizer DS v4. 0. 100. 13345. Accelrys Sof tware Inc (2005).

41. Kaplan W, Littlejohn TG. Swiss-PDB Viewer (Deep View). Briefings in bioinformatics. 2001; 2. https://doi.org/10.1093/bib/2.2.195 PMID: 11465736

42. El-Hachem N, Haibe-Kains B, Khalil A, Kobeissy FH, Nemer G. AutoDock and AutoDockTools for protein-ligand docking: Beta-site amyloid precursor protein cleaving enzyme 1(BACE1) as a case study. Methods in Molecular Biology. 2017. https://doi.org/10.1007/978-1-4939-6952-4_20 PMID: 28508374

43. Hanwell MD, Curtis DE, Lonie DC, Vandermeerschd T, Zurek E, Hutchison GR. Avogadro: An advanced semantic chemical editor, visualization, and analysis platform. Journal of Cheminformatics. 2012; 4. https://doi.org/10.1186/1758-2946-4-17 PMID: 22889332

44. Trott O, Olson AJ. AutoDock Vina: Improving the speed and accuracy of docking with a new scoring function, efficient optimization, and multithreading. Journal of Computational Chemistry. 2009. https://doi.org/10.1002/jcc.21334 PMID: 19499576

45. Krieger Elmar GV, Spronk C. YASARA—Yet Another Scientific Artificial Reality Application. YASARA.org. 2013.

46. Dickson CJ, Madej BD, Skjevik ÅA, Betz RM, Teigen K, Gould IR, et al. Lipid14: The amber lipid force field. Journal of Chemical Theory and Computation. 2014; 10. https://doi.org/10.1021/ct4010307 PMID: 24803855

47. Stewart JJP. MOPAC: A semiempirical molecular orbital program. Journal of Computer-Aided Molecular Design. 1990; 4. https://doi.org/10.1007/BF00128336 PMID: 2197373

48. Jakalian A, Jack DB, Bayly CI. Fast, efficient generation of high-quality atomic charges. AM1-BCC model: II. Parameterization and validation. Journal of Computational Chemistry. 2002; 23. https://doi.org/10.1002/jcc.10128 PMID: 12395429

49. Wang J, Wolf RM, Caldwell JW, Kollman PA, Case DA. Development and testing of a general Amber force field. Journal of Computational Chemistry. 2004; 25. https://doi.org/10.1002/jcc.20035 PMID: 15116359

50. Jorgensen WL, Chandrasekhar J, Madura JD, Impey RW, Klein ML. Comparison of simple potential functions for simulating liquid water. The Journal of Chemical Physics. 1983; 79. https://doi.org/10.1063/1.445869

51. Krieger E, Vriend G. New ways to boost molecular dynamics simulations. Journal of Computational Chemistry. 2015; 36. https://doi.org/10.1002/jcc.23899 PMID: 25824339

52. Krieger E, Nielsen JE, Spronk CAEM, Vriend G. Fast empirical pKa prediction by Ewald summation. Journal of Molecular Graphics and Modelling. 2006; 25. https://doi.org/10.1016/j.jmgm.2006.02.009 PMID: 16644253

53. Hess B, Bekker H, Berendsen HJC, Fraaije JGEM. LINCS: A Linear Constraint Solver for molecular simulations. Journal of Computational Chemistry. 1997; 18. https://doi.org/10.1002/(SICI)1096-987X(199709)18:12<1463::AID-JCC4>3.0.CO;2-H.

54. Miyamoto S, Kollman PA. Settle: An analytical version of the SHAKE and RATTLE algorithm for rigid water models. Journal of Computational Chemistry. 1992; 13. https://doi.org/10.1002/jcc.540130805

55. Essmann U, Perera L, Berkowitz ML, Darden T, Lee H, Pedersen LG. A smooth particle mesh Ewald method. The Journal of Chemical Physics. 1995; 103. https://doi.org/10.1063/1.470117

56. Berendsen HJC, Postma JPM, Van Gunsteren WF, Dinola A, Haak JR. Molecular dynamics with coupling to an external bath. The Journal of Chemical Physics. 1984; 81. https://doi.org/10.1063/1.448118

57. Krieger E, Koraimann G, Vriend G. Increasing the precision of comparative models with YASARA NOVA—A self-parameterizing force field. Proteins: Structure, Function and Genetics. 2002; 47. https://doi.org/10.1002/prot.10104 PMID: 11948792

58. Mitra S, Dash R. Structural dynamics and quantum mechanical aspects of shikonin derivatives as CREBBP bromodomain inhibitors. Journal of Molecular Graphics and Modelling. 2018; 83. https://doi.org/10.1016/j.jmgm.2018.04.014 PMID: 29758466

59. Srinivasan E, Rajasekaran R. Computational investigation of curcumin, a natural polyphenol that inhibits the destabilization and the aggregation of human SOD1 mutant (Ala4Val). RSC Advances. 2016; 6. https://doi.org/10.1039/c6ra21927f

60. Yang L, Xiong H, Li X, Li Y, Zhou H, Lin X, et al. Network Pharmacology and Comparative Transcriptome Reveals Biotargets and Mechanisms of Curcumol Treating Lung Adenocarcinoma Patients With COVID-19. Front Nutr. 2022; 9: 870370. https://doi.org/10.3389/fnut.2022.870370 PMID: 35520289

61. Gu H, Yuan G. Identification of key genes in SARS-CoV-2 patients on bioinformatics analysis. Bioinformatics; 2020 Aug. https://doi.org/10.1101/2020.08.09.243444

62. Hasan MI, Rahman MH, Islam MB, Islam MZ, Hossain MA, Moni MA. Systems Biology and Bioinformatics approach to Identify blood based signatures molecules and drug targets of patient with COVID-19. Informatics in Medicine Unlocked. 2022; 28: 100840. https://doi.org/10.1016/j.imu.2021.100840 PMID: 34981034

63. Gu H, Yuan G. Identification of potential biomarkers and inhibitors for SARS-CoV-2 infection. medRxiv. 2020.

64. Huffman J, Butler-Laporte G, Khan A, Drivas TG, Peloso GM, Nakanishi T, et al. Alternative splicing of OAS1 alters the risk for severe COVID-19. medRxiv. 2021. https://doi.org/10.1101/2021.03.20.21254005 PMID: 33791713

65. Zhou S, Butler-Laporte G, Nakanishi T, Morrison DR, Afilalo J, Afilalo M, et al. A Neanderthal OAS1 isoform protects individuals of European ancestry against COVID-19 susceptibility and severity. Nature medicine. 2021; 27: 659–667. https://doi.org/10.1038/s41591-021-01281-1 PMID: 33633408

66. Magusali N, Graham AC, Piers TM, Panichnantakul P, Yaman U, Shoai M, et al. A genetic link between risk for Alzheimer's disease and severe COVID-19 outcomes via the *OAS1* gene. Brain. 2021; 144: 3727–3741. https://doi.org/10.1093/brain/awab337 PMID: 34619763

67. Schoggins J. Defective Viral Rna Sensing Linked to Severe Covid-19. Science. 2021; 374: 535–536. https://doi.org/10.1126/science.abm3921 PMID: 34709914

68. Salih D. Genetic variability associated with oligoadenylate synthetase 1, OAS1, in myeloid cells increases the risk of Alzheimer's disease and severe COVID-19. Brain and Neuroscience Advances. 2021; 30–31.

69. Chetta M, Rosati A, Marzullo L, Tarsitano M, Bukvic N. A SARS-CoV-2 host infection model network based on genomic human Transcription Factors (TFs) depletion. Heliyon. 2020; 6: e05010. https://doi.org/10.1016/j.heliyon.2020.e05010 PMID: 32984567

70. Uddin M, Loney T, Nowotny N, Alsuwaidi H, Varghese R, Deesi Z, et al. Host transcriptomic profiling of COVID-19 patients with mild, moderate, and severe clinical outcomes. 2020. https://doi.org/10.1016/j.csbj.2020.12.016 PMID: 33425248

71. Lee JS, Park S, Jeong HW, Ahn JY, Choi SJ, Lee H, et al. Immunophenotyping of COVID-19 and influenza highlights the role of type I interferons in development of severe COVID-19. Sci Immunol. 2020; 5: eabd1554. https://doi.org/10.1126/sciimmunol.abd1554 PMID: 32651212

72. Huang J, Zhou X, Gong Y, Chen J, Yang Y, Liu K. Network pharmacology and molecular docking analysis reveals the mechanism of asiaticoside on COVID-19. Annals of Translational Medicine. 2022; 10. https://doi.org/10.21037/atm-22-51 PMID: 35280425

73. Gong B, Huang L, He Y, Xie W, Yin Y, Shi Y, et al. A genetic variant in IL-6 lowering its expression is protective for critical patients with COVID-19. Sig Transduct Target Ther. 2022; 7: 112. https://doi.org/10.1038/s41392-022-00923-1 PMID: 35368020

74. Junior GSM, Kurizky PS, Cerqueira SRPS, Barroso DH, Schulte HL, de Albuquerque CP, et al. Enhanced IL-6 and IL-12B Gene Expression After SARS-CoV-2 Infection in Leprosy Patients May Increase the Risk of Neural Damage. The American Journal of Tropical Medicine and Hygiene. 2021; 104: 2190. https://doi.org/10.4269/ajtmh.21-0034 PMID: 33819170

75. Santa Cruz A, Mendes-Frias A, Oliveira AI, Dias L, Matos AR, Carvalho A. Interleukin-6 is a biomarker for the development of fatal severe acute respiratory syndrome coronavirus 2 pneumonia. Front Immunol. 2021; 12: 613422. 2021. https://doi.org/10.3389/fimmu.2021.613422 PMID: 33679753

76. Ascierto PA, Fu B, Wei H. IL-6 modulation for COVID-19: the right patients at the right time? Journal for immunotherapy of cancer. 2021; 9. https://doi.org/10.1136/jitc-2020-002285 PMID: 33837054

77. Luo W, Ding R, Guo X, Zhan T, Tang T, Fan R, et al. Clinical data mining reveals Gancao-Banxia as a potential herbal pair against moderate COVID-19 by dual binding to IL-6/STAT3. Computers in biology and medicine. 2022; 145: 105457. https://doi.org/10.1016/j.compbiomed.2022.105457 PMID: 35366469

78. Bovijn J, Lindgren CM, Holmes MV. Genetic IL-6R variants and therapeutic inhibition of IL-6 receptor signalling in COVID-19–Authors' reply. The Lancet Rheumatology. 2021; 3: e97–e98. https://doi.org/10.1016/S2665-9913(20)30415-X PMID: 33521676

79. Niu W, Wu F, Cao W, Wu Z, Chao Y-C, Peng F, et al. Network pharmacology for the identification of phytochemicals in traditional Chinese medicine for COVID-19 that may regulate interleukin-6. Bioscience Reports. 2021; 41. https://doi.org/10.1042/BSR20202583 PMID: 33146673

80. Kumar S. COVID-19: A drug repurposing and biomarker identification by using comprehensive gene-disease associations through protein-protein interaction network analysis. 2020.

81. Mondeali M, Bemani P, Hosseini P, Kesheh MM, Bahavar A. Comparative Transcriptomic Analysis Be-tween SARS-COV-2, RSV And Influenza H3N2 Patients Highlights The Use Of IL-6 Inhibitors. J Bioinfo Comp Genom. 2022; 5: 1–15.

82. Giamarellos-Bourboulis EJ, Netea MG, Rovina N, Akinosoglou K, Antoniadou A, Antonakos N, et al. Complex immune dysregulation in COVID-19 patients with severe respiratory failure. Cell host & microbe. 2020; 27: 992–1000. https://doi.org/10.1016/j.chom.2020.04.009 PMID: 32320677

83. Huang J, Wang Y, Zha Y, Zeng X, Li W, Zhou M. Transcriptome Analysis Reveals Hub Genes Regulating Autophagy in Patients With Severe COVID-19. Frontiers in Genetics. 2022; 13. https://doi.org/10.3389/fgene.2022.908826 PMID: 35923698

84. Shen Y-A, Jung J, Shimberg GD, Hsu F-C, Rahmanto YS, Gaillard SL, et al. Development of small molecule inhibitors targeting PBX1 transcription signaling as a novel cancer therapeutic strategy. Iscience. 2021; 24: 103297. https://doi.org/10.1016/j.isci.2021.103297 PMID: 34816098

85. Fang C, Mei J, Tian H, Liou Y-L, Rong D, Zhang W, et al. CSF3 is a potential drug target for the treatment of COVID-19. Frontiers in Physiology. 2021; 11: 605792. https://doi.org/10.3389/fphys.2020.605792 PMID: 33551833

86. Zhou Y, Hou Y, Shen J, Huang Y, Martin W, Cheng F. Network-based drug repurposing for novel coronavirus 2019-nCoV/SARS-CoV-2. Cell discovery. 2020; 6: 1–18.

87. Laha S, Saha C, Dutta S, Basu M, Chatterjee R, Ghosh S, et al. In silico analysis of altered expression of long non-coding RNA in SARS-CoV-2 infected cells and their possible regulation by STAT1, STAT3 and interferon regulatory factors. Heliyon. 2021; 7: e06395. https://doi.org/10.1016/j.heliyon.2021.e06395 PMID: 33688586

88. Selvaraj G, Kaliamurthi S, Peslherbe GH, Wei D-Q. Identifying potential drug targets and candidate drugs for COVID-19: biological networks and structural modeling approaches. F1000Research. 2021; 10. https://doi.org/10.12688/f1000research.50850.3 PMID: 33968364

89. Yang C, Dou R, Yin T, Ding J. MiRNA-106b-5p in human cancers: diverse functions and promising biomarker. Biomedicine & Pharmacotherapy. 2020; 127: 110211. https://doi.org/10.1016/j.biopha.2020.110211 PMID: 32422566

90. Khan M, Sany M, Us R, Islam M, Islam ABMM. Epigenetic regulator miRNA pattern differences among SARS-CoV, SARS-CoV-2, and SARS-CoV-2 world-wide isolates delineated the mystery behind the epic pathogenicity and distinct clinical characteristics of pandemic COVID-19. Frontiers in genetics. 2020; 765.

91. Liang L, Zhao L, Zan Y, Zhu Q, Ren J, Zhao X. MiR-93-5p enhances growth and angiogenesis capacity of HUVECs by down-regulating EPLIN. Oncotarget. 2017; 8: 107033. https://doi.org/10.18632/oncotarget.22300 PMID: 29291009

92. Khokhar M, Tomo S, Purohit P. MicroRNAs based regulation of cytokine regulating immune expressed genes and their transcription factors in COVID-19. Meta gene. 2022; 31: 100990. https://doi.org/10.1016/j.mgene.2021.100990 PMID: 34722158

93. Sardar R, Satish D, Gupta D. Identification of novel SARS-CoV-2 drug targets by host microRNAs and transcription factors co-regulatory interaction network analysis. Frontiers in Genetics. 2020; 11: 1105. https://doi.org/10.3389/fgene.2020.571274 PMID: 33173539

94. Angriman F, Ferreyro BL, Burry L, Fan E, Ferguson ND, Husain S, et al. Interleukin-6 receptor blockade in patients with COVID-19: placing clinical trials into context. The Lancet Respiratory Medicine. 2021; 9: 655–664. https://doi.org/10.1016/S2213-2600(21)00139-9 PMID: 33930329

95. Netherton CL, Wileman T. Virus factories, double membrane vesicles and viroplasm generated in animal cells. Current opinion in virology. 2011; 1: 381–387. https://doi.org/10.1016/j.coviro.2011.09.008 PMID: 22440839

96. Sabaka P, Koščálová A, Straka I, Hodosy J, Lipták R, Kmotorková B, et al. Role of interleukin 6 as a predictive factor for a severe course of Covid-19: retrospective data analysis of patients from a long-term care facility during Covid-19 outbreak. BMC infectious diseases. 2021; 21: 1–8.

97. Murugan NA, Kumar S, Jeyakanthan J, Srivastava V. Searching for target-specific and multi-targeting organics for Covid-19 in the Drugbank database with a double scoring approach. Scientific reports. 2020; 10: 1–16.

98. de Oliveira OV, Rocha GB, Paluch AS, Costa LT. Repurposing approved drugs as inhibitors of SARS-CoV-2 S-protein from molecular modeling and virtual screening. Journal of Biomolecular Structure and Dynamics. 2021; 39: 3924–3933.

99. Cagno V, Magliocco G, Tapparel C, Daali Y. The tyrosine kinase inhibitor nilotinib inhibits SARS-CoV-2 in vitro. Basic & clinical pharmacology & toxicology. 2021; 128: 621–624. https://doi.org/10.1111/bcpt.13537 PMID: 33232578

100. Bouchlarhem A, Haddar L, Lamzouri O, Nasri S, Aichouni N, Bkiyar H, et al. Multiple cranial nerve palsies revealing blast crisis in patient with chronic myeloid leukemia in the accelerated phase under nilotinib during severe infection with SARS-COV-19 virus: case report and review of literature. Radiology Case Reports. 2021; 16: 3602–3609. https://doi.org/10.1016/j.radcr.2021.08.030 PMID: 34422148

101. Banerjee S, Yadav S, Banerjee S, Fakayode SO, Parvathareddy J, Reichard W, et al. Drug repurposing to identify nilotinib as a potential SARS-CoV-2 main protease inhibitor: insights from a computational and in vitro study. Journal of chemical information and modeling. 2021; 61: 5469–5483. https://doi.org/10.1021/acs.jcim.1c00524 PMID: 34666487

102. Heidari A, Caissutti A, Henderson M, Schmitt K, Besana E, Esposito J, et al. Recent New Results and Achievements of California South University (CSU) BioSpectroscopy Core Research Laboratory for COVID-19 or 2019-nCoV Treatment: Diagnosis and Treatment Methodologies of "Coronavirus. Journal of Current Viruses and Treatment Methodologies. 2020; 1: 3–41.

103. Ruan Z, Liu C, Guo Y, He Z, Huang X, Jia X, et al. SARS-CoV-2 and SARS-CoV: Virtual screening of potential inhibitors targeting RNA-dependent RNA polymerase activity (NSP12). Journal of medical virology. 2021; 93: 389–400. https://doi.org/10.1002/jmv.26222 PMID: 32579254

104. Chandel V, Sharma PP, Raj S, Choudhari R, Rathi B, Kumar D. Structure-based drug repurposing for targeting Nsp9 replicase and spike proteins of severe acute respiratory syndrome coronavirus 2. Journal of Biomolecular Structure and Dynamics. 2022; 40: 249–262. https://doi.org/10.1080/07391102.2020.1811773 PMID: 32838660

105. Li Y, Zhang J, Wang N, Li H, Shi Y, Guo G, et al. Therapeutic drugs targeting 2019-nCoV main protease by high-throughput screening. BioRxiv. 2020.

106. Encinar JA, Menendez JA. Potential drugs targeting early innate immune evasion of SARS-coronavirus 2 via 2'-O-methylation of viral RNA. Viruses. 2020; 12: 525. https://doi.org/10.3390/v12050525 PMID: 32397643

107. Sahoo BM, Ravi Kumar BVV, Sruti J, Mahapatra MK, Banik BK, Borah P. Drug repurposing strategy (DRS): Emerging approach to identify potential therapeutics for treatment of novel coronavirus infection. Frontiers in Molecular Biosciences. 2021; 8: 628144. https://doi.org/10.3389/fmolb.2021.628144 PMID: 33718434

108. Ruan Z, Liu C, Guo Y, He Z, Huang X, Jia X, et al. Potential inhibitors targeting RNA-dependent RNA polymerase activity (NSP12) of SARS-CoV-2. 2020.

109. Zhou Y-W, Xie Y, Tang L-S, Pu D, Zhu Y-J, Liu J-Y, et al. Therapeutic targets and interventional strategies in COVID-19: mechanisms and clinical studies. Signal transduction and targeted therapy. 2021; 6: 1–25.

110. Cho J, Lee YJ, Kim JH, Kim SS, Choi B-S, Choi J-H. Antiviral activity of digoxin and ouabain against SARS-CoV-2 infection and its implication for COVID-19. Scientific reports. 2020; 10: 1–8.

111. Xing Y, Yin L, Guo M, Shi H, Qi T, Wang L, et al. Therapeutic Monitoring of Plasma Digoxin for COVID-19 Patients Using a Simple UPLC-MS/MS Method. Current Pharmaceutical Analysis. 2021; 17: 1308–1316.

112. Peltzer B, Lerman BB, Goyal P, Cheung JW. Role for digoxin in patients hospitalized with COVID-19 and atrial arrhythmias. Journal of Cardiovascular Electrophysiology. 2021; 32: 880. https://doi.org/10.1111/jce.14901 PMID: 33522631

113. Rattanawong P, Shen W, El Masry H, Sorajja D, Srivathsan K, Valverde A, et al. Guidance on short-term management of atrial fibrillation in coronavirus disease 2019. Journal of the American Heart Association. 2020; 9: e017529. https://doi.org/10.1161/JAHA.120.017529 PMID: 32515253

114. Talluri S. Molecular docking and virtual screening based prediction of drugs for COVID-19. Combinatorial Chemistry & High Throughput Screening. 2021; 24: 716–728. https://doi.org/10.2174/1386207323666200814132149 PMID: 32798373

115. Sekhar T. Virtual Screening based prediction of potential drugs for COVID-19. Combinatorial Chemistry & High Throughput Screening. 2020; 23.

116. Aishwarya S, Gunasekaran K, Margret AA. Computational gene expression profiling in the exploration of biomarkers, non-coding functional RNAs and drug perturbagens for COVID-19. Journal of Biomolecular Structure and Dynamics. 2020; 1–16. https://doi.org/10.1080/07391102.2020.1850360 PMID: 33228475

117. Xu J, Xue Y, Zhou R, Shi P, Li H, Zhou J. Drug repurposing approach to combating coronavirus: Potential drugs and drug targets. Med Res Rev. 2021; 41: 1375–1426. https://doi.org/10.1002/med.21763 PMID: 33277927

118. Jeon S, Ko M, Lee J, Choi I, Byun SY, Park S, et al. Identification of Antiviral Drug Candidates against SARS-CoV-2 from FDA-Approved Drugs. Antimicrob Agents Chemother. 2020; 64: e00819–20. https://doi.org/10.1128/AAC.00819-20 PMID: 32366720

119. Mosharaf MdP Kibria MdK, Hossen MdB Islam MdA, Reza MdS Mahumud RA, et al. Meta-Data Analysis to Explore the Hub of the Hub-Genes That Influence SARS-CoV-2 Infections Highlighting Their Pathogenetic Processes and Drugs Repurposing. Vaccines. 2022; 10: 1248. https://doi.org/10.3390/vaccines10081248 PMID: 36016137

120. Feng Z, Chen M, Liang T, Shen M, Chen H, Xie X-Q. Virus-CKB: an integrated bioinformatics platform and analysis resource for COVID-19 research. Briefings in Bioinformatics. 2021; 22: 882–895. https://doi.org/10.1093/bib/bbaa155 PMID: 32715315

121. Feng Z, Chen M, Xue Y, Liang T, Chen H, Zhou Y, et al. MCCS: a novel recognition pattern-based method for fast track discovery of anti-SARS-CoV-2 drugs. Briefings in Bioinformatics. 2021; 22: 946–962. https://doi.org/10.1093/bib/bbaa260 PMID: 33078827

122. Ruan Z, Liu C, Guo Y, He Z, Huang X, Jia X, et al. SARS-CoV-2 and SARS-CoV: Virtual screening of potential inhibitors targeting RNA-dependent RNA polymerase activity (NSP12). J Med Virol. 2021; 93: 389–400. https://doi.org/10.1002/jmv.26222 PMID: 32579254

123. Jamalipour Soufi G, Iravani S. Potential inhibitors of SARS-CoV-2: recent advances. Journal of Drug Targeting. 2021; 29: 349–364. https://doi.org/10.1080/1061186X.2020.1853736 PMID: 33210953

124. Lo HS, Hui KPY, Lai H-M, He X, Khan KS, Kaur S, et al. Simeprevir potently suppresses SARS-CoV-2 replication and synergizes with remdesivir. ACS central science. 2021; 7: 792–802. https://doi.org/10.1021/acscentsci.0c01186 PMID: 34075346

125. J A, Francis D, C.S S, K.G A, C S, Variyar EJ. Repurposing simeprevir, calpain inhibitor IV and a cathepsin F inhibitor against SARS-CoV-2 and insights into their interactions with M ^{pro}. Journal of Biomolecular Structure and Dynamics. 2022; 40: 325–336. https://doi.org/10.1080/07391102.2020.1813200 PMID: 32873185

126. Behera S, Mahapatra N, Tripathy C, Pati S. Drug repurposing for identification of potential inhibitors against SARS-CoV-2 spike receptor-binding domain: An in silico approach. Indian J Med Res. 2021; 153: 132. https://doi.org/10.4103/ijmr.IJMR_1132_20 PMID: 33818470

127. Kadioglu O, Saeed M, Greten HJ, Efferth T. Identification of novel compounds against three targets of SARS CoV-2 coronavirus by combined virtual screening and supervised machine learning. Computers in Biology and Medicine. 2021; 133: 104359. https://doi.org/10.1016/j.compbiomed.2021.104359 PMID: 33845270

128. Khan RJ, Jha RK, Singh E, Jain M, Amera GM, Singh RP, et al. Identification of promising antiviral drug candidates against non-structural protein 15 (NSP15) from SARS-CoV-2: an in silico assisted drug-repurposing study. Journal of Biomolecular Structure and Dynamics. 2022; 40: 438–448. https://doi.org/10.1080/07391102.2020.1814870 PMID: 32885740

129. Cheng F-J, Huynh T-K, Yang C-S, Hu D-W, Shen Y-C, Tu C-Y, et al. Hesperidin Is a Potential Inhibitor against SARS-CoV-2 Infection. Nutrients. 2021; 13: 2800. https://doi.org/10.3390/nu13082800 PMID: 34444960

130. Bellavite P, Donzelli A. Hesperidin and SARS-CoV-2: New light on the healthy function of citrus fruits. Antioxidants. 2020; 9: 742. https://doi.org/10.3390/antiox9080742 PMID: 32823497

131. Das S, Sarmah S, Lyndem S, Singha Roy A. An investigation into the identification of potential inhibitors of SARS-CoV-2 main protease using molecular docking study. Journal of Biomolecular Structure and Dynamics. 2020; 1–11. https://doi.org/10.1080/07391102.2020.1763201 PMID: 32362245

132. Wu C, Liu Y, Yang Y, Zhang P, Zhong W, Wang Y, et al. Analysis of therapeutic targets for SARS-CoV-2 and discovery of potential drugs by computational methods. Acta Pharmaceutica Sinica B. 2020; 10: 766–788. https://doi.org/10.1016/j.apsb.2020.02.008 PMID: 32292689

133. Balmeh N, Mahmoudi S, Mohammadi N, Karabedianhajiabadi A. Predicted therapeutic targets for COVID-19 disease by inhibiting SARS-CoV-2 and its related receptors. Informatics in Medicine Unlocked. 2020; 20: 100407. https://doi.org/10.1016/j.imu.2020.100407 PMID: 32835083

134. Matondo A, Kilembe JT, Ngoyi EM, Kabengele CN, Kasiama GN, Lengbiye EM, et al. Oleanolic Acid, Ursolic Acid and Apigenin from Ocimum basilicum as Potential Inhibitors of the SARS-CoV-2 Main Protease: A Molecular Docking Study. IJPR. 2021; 1–16. https://doi.org/10.9734/ijpr/2021/v6i230156

135. Kumar A, Choudhir G, Shukla SK, Sharma M, Tyagi P, Bhushan A, et al. Identification of phytochemical inhibitors against main protease of COVID-19 using molecular modeling approaches. Journal of Biomolecular Structure and Dynamics. 2021; 39: 3760–3770. https://doi.org/10.1080/07391102.2020.1772112 PMID: 32448034

136. Fitriani IN, Utami W, Zikri AT, Santoso P. In Silico Approach of Potential Phytochemical Inhibitor from Moringa oleifera, Cocos nucifera, Allium cepa, Psidium guajava, and Eucalyptus globulus for the treatment of COVID-19 by Molecular Docking. In Review; 2020 Jul. https://doi.org/10.21203/rs.3.rs-42747/v1

137. Chen H, Zhang Z, Wang L, Huang Z, Gong F, Li X, et al. First clinical study using HCV protease inhibitor danoprevir to treat COVID-19 patients. Medicine (Baltimore). 2020; 99: e23357. https://doi.org/10.1097/MD.0000000000023357 PMID: 33235105

138. Zhang Z, Wang S, Tu X, Peng X, Huang Y, Wang L, et al. A comparative study on the time to achieve negative nucleic acid testing and hospital stays between danoprevir and lopinavir/ritonavir in the treatment of patients with COVID-19. J Med Virol. 2020; 92: 2631–2636. https://doi.org/10.1002/jmv.26141 PMID: 32501538

139. Liu J, Zhai Y, Liang L, Zhu D, Zhao Q, Qiu Y. Molecular modeling evaluation of the binding effect of five protease inhibitors to COVID-19 main protease. Chem Phys. 2021; 542: 111080. https://doi.org/10.1016/j.chemphys.2020.111080 PMID: 33519023

140. Jonny, Violetta L, Kartasasmita AS, Amirullah Roesli RM, Rita C. Pharmacological Treatment Options for Coronavirus Disease-19 in Renal Patients. Uribarri J, editor. International Journal of Nephrology. 2021; 2021: 1–9. https://doi.org/10.1155/2021/4078713 PMID: 34858665

141. Santos-Filho OA. Identification of Potential Inhibitors of Severe Acute Respiratory Syndrome-Related Coronavirus 2 (SARS-CoV-2) Main Protease from Non-Natural and Natural Sources: A Molecular Docking Study. SciELO journals; 2021. p. 1428671 Bytes. https://doi.org/10.6084/M9.FIGSHARE.14304102.V1

142. Teoh SL, Lim YH, Lai NM, Lee SWH. Directly Acting Antivirals for COVID-19: Where Do We Stand? Front Microbiol. 2020; 11: 1857. https://doi.org/10.3389/fmicb.2020.01857 PMID: 32849448

143. Lotfi M, Hamblin MR, Rezaei N. COVID-19: Transmission, prevention, and potential therapeutic opportunities. Clinica Chimica Acta. 2020; 508: 254–266. https://doi.org/10.1016/j.cca.2020.05.044 PMID: 32474009

144. Beck BR, Shin B, Choi Y, Park S, Kang K. Predicting commercially available antiviral drugs that may act on the novel coronavirus (SARS-CoV-2) through a drug-target interaction deep learning model. Computational and Structural Biotechnology Journal. 2020; 18: 784–790. https://doi.org/10.1016/j.csbj.2020.03.025 PMID: 32280433

145. Lovering AL, Seung SL, Kim YW, Withers SG, Strynadka NCJ. Mechanistic and structural analysis of a family 31 α-glycosidase and its glycosyl-enzyme intermediate. Journal of Biological Chemistry. 2005; 280. https://doi.org/10.1074/jbc.M410468200 PMID: 15501829

146. Blatt JM, Weisskopf VF, Critchfield CL. Theoretical Nuclear Physics. American Journal of Physics. 1953; 21. https://doi.org/10.1119/1.1933407